Atmos. Chem. Phys., 13, 11101–11120, 2013
www.atmos-chem-phys.net/13/11101/2013/
doi:10.5194/acp-13-11101-2013

Atmospheric Chemistry and Physics Open Access

Constraints on emissions of carbon monoxide, methane, and a suite of hydrocarbons in the Colorado Front Range using observations of $^{14}CO_2$

B. W. LaFranchi[1], G. Pétron[2,3], J. B. Miller[2,3], S. J. Lehman[4], A. E. Andrews[2], E. J. Dlugokencky[2], B. Hall[2], B. R. Miller[2,3], S. A. Montzka[2], W. Neff[3,5], P. C. Novelli[2], C. Sweeney[2,3], J. C. Turnbull[3,6], D. E. Wolfe[5], P. P. Tans[2], K. R. Gurney[7], and T. P. Guilderson[1]

[1]Center for Accelerator Mass Spectrometry (CAMS), Lawrence Livermore National Laboratory, Livermore, CA 94550, USA
[2]Global Monitoring Division (GMD), NOAA Earth System Research Laboratory, Boulder, CO 80305, USA
[3]Cooperative Institute for Research in Environmental Sciences (CIRES), University of Colorado, Boulder CO 80309, USA
[4]Institute for Arctic and Alpine Research (INSTAAR), University of Colorado, Boulder 80305, USA
[5]Physical Sciences Division, NOAA Earth System Research Laboratory, Boulder, CO 80305, USA
[6]National Isotope Centre, GNS Science, Lower Hutt 5040, New Zealand
[7]School of Life Sciences, Arizona State University, Tempe, AZ 85287, USA

Correspondence to: B. W. LaFranchi (lafranchi2@llnl.gov)

Received: 6 December 2012 – Published in Atmos. Chem. Phys. Discuss.: 15 January 2013
Revised: 17 August 2013 – Accepted: 4 September 2013 – Published: 15 November 2013

Abstract. Atmospheric radiocarbon (^{14}C) represents an important observational constraint on emissions of fossil-fuel derived carbon into the atmosphere due to the absence of ^{14}C in fossil fuel reservoirs. The high sensitivity and precision that accelerator mass spectrometry (AMS) affords in atmospheric ^{14}C analysis has greatly increased the potential for using such measurements to evaluate bottom-up emissions inventories of fossil fuel CO_2 (CO_2ff), as well as those for other co-emitted species. Here we use observations of $^{14}CO_2$ and a series of primary hydrocarbons and combustion tracers from discrete air samples collected between June 2009 and September 2010 at the National Oceanic and Atmospheric Administration Boulder Atmospheric Observatory (BAO; Lat: 40.050° N, Lon: 105.004° W) to derive emission ratios of each species with respect to CO_2ff. The BAO tower is situated at the boundary of the Denver metropolitan area to the south and a large industrial and agricultural region to the north and east, making it an ideal location to study the contrasting mix of emissions from the activities in each region. The species considered in this analysis are carbon monoxide (CO), methane (CH_4), acetylene (C_2H_2), benzene (C_6H_6), and C_3–C_5 alkanes. We estimate emissions for a subset of these species by using the Vulcan high resolution CO_2ff emission data product as a reference. We find that CO is overestimated in the 2008 National Emissions Inventory (NEI08) by a factor of ∼2. A close evaluation of the inventory suggests that the ratio of CO emitted per unit fuel burned from on-road gasoline vehicles is likely over-estimated by a factor of 2.5. Using a wind-directional analysis of the data, we find enhanced concentrations of CH_4, relative to CO_2ff, in air influenced by emissions to the north and east of the BAO tower when compared to air influenced by emissions in the Denver metro region to the south. Along with enhanced CH_4, the strongest enhancements of the C_3–C_5 alkanes are also found in the north and east wind sector, suggesting that both the alkane and CH_4 enhancements are sourced from oil and gas fields located to the northeast, though it was not possible to rule out the contribution of non oil and gas CH_4 sources.

1 Introduction

The relative abundance of radiocarbon (^{14}C) in CO_2 ($^{14}CO_2$) is a powerful tracer that provides the least biased and most direct means to observe fossil fuel derived CO_2 in the atmosphere (Zondervan and Meijer, 1996; Levin et al., 2003;

Turnbull et al., 2006; Hsueh et al., 2007; Levin and Karstens, 2007; Turnbull et al., 2009; Van der Laan et al., 2010). Fossil fuels are completely devoid of ^{14}C, as is the CO_2 resulting from its combustion, because the half life of ^{14}C is short (∼5700 yr; Godwin, 1962) in relation to the residence times of carbon in fossil reservoirs, where no additional ^{14}C production occurs. Since all other sources of CO_2 to the atmosphere stem from carbon reservoirs (the ocean and biosphere) that are nearly in equilibrium with the isotopic composition of the atmosphere itself, the atmosphere exhibits gradients in $^{14}CO_2$ that can be quantitatively traced to addition of CO_2 from fossil fuel combustion (Turnbull et al., 2007; Graven et al., 2009; Levin et al., 2010).

Prior to nuclear weapons testing, which artificially increased the $^{14}CO_2$ content of the atmosphere, the rise in atmospheric CO_2 resulting from fossil fuel combustion could be observed on global scales as a decrease in $^{14}CO_2$, widely known as the Suess effect (Suess, 1955). While $^{14}CO_2$ is produced naturally in the upper atmosphere from cosmogenic radiation, the abundance of $^{14}CO_2$ in the modern atmosphere was strongly impacted by above-ground nuclear testing that occurred in the middle part of the 20th century. Since the atmospheric nuclear weapons test ban was put in place, the decrease in $^{14}CO_2$, which has been observed at a number of global background monitoring sites (Levin and Kromer, 2004; Turnbull et al., 2007; Currie et al., 2011; Graven et al., 2012a, b; Lehman et al., 2013), has been influenced primarily by the exchange of atmospheric $^{14}CO_2$ with the oceanic and terrestrial carbon reservoirs. In recent years, however, the atmospheric decline has been increasingly influenced by isotopic dilution due to the Seuss effect, as fossil fuel combustion increases and as the atmosphere, ocean, and terrestrial carbon reservoirs approach equilibrium with the "bomb spike". On regional scales, locally emitted CO_2 from fossil fuel combustion can be detected as a depletion of ^{14}C:^{12}C relative to background air. These observed gradients result from what we define as "recently added" fossil-fuel CO_2 (CO_2ff).

Observations of $^{14}CO_2$ downwind of source regions are of great interest, not only for the evaluation of fossil CO_2 emissions inventories, but also as a means to better understand emissions of a range of trace gases associated or co-located with the combustion of fossil fuels (Turnbull et al., 2011; Miller et al., 2012). Bottom-up inventories of these trace gases carry significant uncertainties because of the difficulty in quantifying the relationship between the mass of fuel consumed and the mass of trace gas emitted. Emissions of by-products, including species such as carbon monoxide (CO), methane (CH_4), acetylene (C_2H_2), and benzene (C_6H_6) depend on a number of variables including fuel type, combustion temperature, the extent of tail-pipe or flue-stack "scrubbing", and oxidant-to-fuel ratio. For example, it has long been known from observations that the National Emissions Inventory (NEI) appears to over-estimate observed anthropogenic emissions of CO in the United States by a factor of ∼1.5–2 (Parrish, 2006; Hudman et al., 2008; Miller et al., 2008, 2012). Further, there are a number of industrial activities that lead to non-combustion emissions of gases impacting air quality and climate from leaks in transmission lines, venting of storage tanks, and other processes, in which case, quantifying emissions based on readily available fuel use, production, or activity statistics can lead to large uncertainties. In contrast, the amount of CO_2 emitted per unit of fuel combusted can be derived stoichiometrically with relatively high accuracy. Accordingly, the bottom-up inventory of fossil fuel derived CO_2 in the United States (e.g. EPA, 2012) and in most developed countries is thought to be relatively reliable. Estimates of annual fossil CO_2 emissions for developed countries are thought to be reliable to better than ∼8 % (Nassar et al., 2013), although uncertainties become larger at smaller spatial and temporal scales (Andres et al., 2012).

Atmospheric observations provide a direct means of improving emissions estimates for various combustion and industrial tracers and of evaluating existing bottom-up emissions estimates, and is especially important for those species that can affect air quality, human health, and climate. One relatively simple strategy for deriving emissions based on atmospheric observations is the use of tracer/tracer enhancement ratios in which emission ratios of two well-correlated species are inferred from the ratio of the observed mole fraction enhancements (with respect to background observations) of one species to the other. For gases with lifetimes comparable to the transit times between emission and measurement, a simple photochemical age model can be used to extrapolate back from the time of the observation to derive the ratio at the time of emission (Lee et al., 2006; Warneke et al., 2007). Then, if emissions of one of the tracers are relatively well defined for the geographic area that the observations are sensitive to, emissions of the other tracer can be calculated from the inferred emission ratio. Uncertainties for this method are minimized when both tracers have long atmospheric lifetimes and slow atmospheric production rates on the time scales relevant to the source-receptor distances. A major advantage of this approach comes from its computational simplicity. Additionally, since all tracers are expected to be mixed and transported in the same way if their sources are co-located, this approach reduces the sensitivity of the analysis on uncertainties in transport and boundary layer calculations.

The Vulcan high resolution fossil fuel CO_2 data product (Gurney et al., 2009) provides an ideal reference emissions dataset for use in these tracer/tracer approaches at local-to-regional scales, but large uncertainties in its biogenic sources and sinks can complicate the use of CO_2 in inferring emissions of other fossil fuel combustion tracers (e.g. Miller et al., 2012). Thus, to take advantage of the photochemical stability of CO_2 and the availability of the relatively accurate fossil fuel CO_2 emissions inventories, measurements of $^{14}CO_2$ can be used to isolate the fossil fuel contribution to the observed

CO_2. Here we describe observations of $^{14}CO_2$ and other trace gases made between late June 2009 and September 2010 at the Boulder Atmospheric Observatory (BAO), a 300 m tall tower located 35 km north of Denver, CO (Lat 40.05° N, Lon 105.01° W) in Weld County. BAO is one of 9 towers in the NOAA Earth System Research Laboratory, Global Monitoring Division (NOAA-GMD, hereinafter) tall tower network (Andrews et al., 2013). It is one of 7 towers in the network that is monitoring CO_2 and CO continuously and collecting air samples daily for multiple species analysis and one of 6 that also measures $^{14}CO_2$ in discrete air samples. The observations presented here represent the first report of $^{14}CO_2$ observations from this network.

This study builds on a previous effort to characterize emissions of volatile organic compounds (VOCs) and CH_4 from oil and gas production and drilling operations in Weld County using both bottom-up and top-down approaches for 2008 (Pétron et al., 2012). We will refer to this prior study as the Colorado Front Range Pilot Study (CFRPS, hereafter), in which the authors made use of observations at BAO in combination with those from a mobile platform to determine emission magnitudes and emission signatures of individual methane sources, including oil and gas wells, natural gas processing plants, condensate storage tanks, landfills, cattle feed-lots, and waste water treatment plants. Continuous wind measurements at BAO enabled wind-sector specific analyses of atmospheric composition, which showed that trace gas concentrations measured at BAO are influenced most substantially by two different source regions: oil and gas fields to the northeast (from a region known as the Denver Julesberg Basin, or DJB) and urban-type emissions from the Denver metro region to the south. They found that air arriving at BAO from the northeast exhibits strong enhancements in alkanes, including methane, resembling enhancements (based on tracer/tracer ratios) similar to those sampled on the mobile platform within the DJB. These results suggested that oil and gas operations are the dominant emitters of alkanes, including methane in the region.

In this study, we use $^{14}CO_2$ to derive CO_2ff mole fractions and show that CO_2ff exhibits strong correlations with a variety of trace gases in the region, both from combustion and non-combustion sources, allowing for the evaluation of emissions from a range of different source-types. We estimate emission ratios for a number of important trace gases being transported to the site from the DJB as well as from the Denver metro region. The variability in tracer/CO_2ff ratios with wind direction is analyzed in order to evaluate regional differences in emission sources, relative to CO_2ff sources. For the trace gases related to the oil and gas industry, which exhibit strong wind-direction dependent enhancement ratios relative to CO_2ff, deriving emissions estimates is challenging due to uncertainty in the precise geographical area of emissions that the observations are sensitive to. In the cases of CO and C_2H_2, however, it is shown that the emission ratio is insensitive to the presumed area of emissions influencing the observations, and top-down emissions for these two tracers can be reliably estimated for the region. The primary advantage of this approach is that by using the Vulcan data product (Gurney et al., 2009) as a quantitative reference, which is reliable nationwide to within 20 % at the county level on annual time-scales (Gurney et al., 2011), we maximize confidence in the derived top-down emission magnitudes.

2 Methods

2.1 Site description

The BAO tower is located 25 km east-northeast of Boulder and 35 km north of Denver (40.05° N, 105.01° W). The base of the tower is at 1584 m above sea level (a.s.l.). As shown in Fig. 1, BAO is located at the southwestern edge of the DJB where a very large and dense network of oil and gas wells exists. Since late 2007 NOAA-GMD has been collecting discrete air samples approximately daily from 300 m. The air is collected in glass flasks and analyzed at NOAA-GMD for a suite of ∼50 trace gases and then circulated to the University of Colorado's Institute of Arctic and Alpine Research (INSTAAR) for stable isotope measurements in CO_2 and CH_4 and preparation for $^{14}CO_2$ measurement. The Center for Accelerator Mass Spectrometry (CAMS) at Lawrence Livermore National Laboratory (LLNL), which performed the $^{14}CO_2$ measurements reported here, has participated in the NOAA-GMD $^{14}CO_2$ discrete air sample measurement program since 2009. This study focuses on data collected between late June 2009 and September 2010, over which time 145 samples were analyzed for $^{14}CO_2$. More information on this site and the entire tall tower network can be found at: http://www.esrl.noaa.gov/gmd/ccgg/towers/.

Standard meteorological measurements are also made continuously at several levels (10 m, 100 m, and 300 m, reported at 60 s, 60 s, and 30 s, respectively)) on the tower by the NOAA ESRL Physical Sciences Division (NOAA-PSD), including wind speed and direction, relative humidity, and temperature. We categorize each observation in our analysis according to wind direction (at 300 m) to facilitate a discussion of two distinct emission source regions: the oil and gas industrial region to the north and east and the Denver metro region to the south. To do this, we define three wind sectors, consistent with those defined in the CFRPS: N/E (345° to 120°), S (120° to 240°), and W (240° to 345°). These wind sectors are illustrated in Fig. 1. Wind sector boundaries are defined based on an analysis of the CH_4/CO_2ff ratio variability with wind direction, which shows two distinct regimes for the CH_4/CO_2ff ratio (see Sect. 3.2). Wind direction for each sample is determined using the mean wind direction over the 30 minutes immediately prior to sampling. Samples with mean wind speeds lower than 2.5 m s^{-1} over this time period are removed from any sector-specific analysis in this study, in order to reduce the number of samples carrying

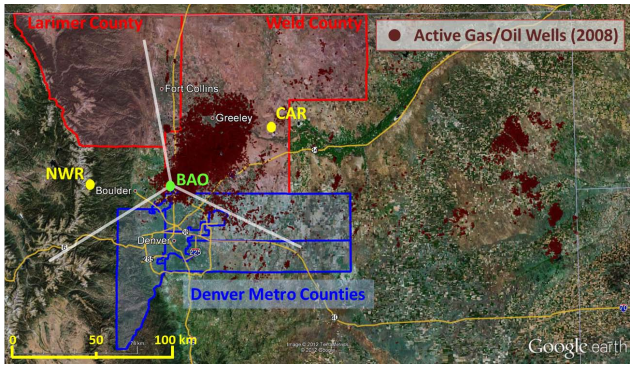

Fig. 1. Map of northeast Colorado showing the BAO tower and the distribution of active oil and gas wells as of 2008 (updated well locations available at: http://cogcc.state.co.us/Home/gismain.cfm). Two background sites are also shown: Niwot Ridge (NWR; 3523 m a.s.l.) and the Briggsdale aircraft site (CAR). Also shown are the three wind sectors used to filter the dataset for emission estimates in Weld/Larimer counties (North and East) and in the Denver metro counties (South). The Denver metro counties include Denver, Broomfield, Adams, Arapahoe, and Jefferson. Top left corner of this map is: 41.064° N, 106.248° W.

a disproportionate influence from sources in the immediate vicinity of the tower. Using a filter of greater than 2.5 m s^{-1} leaves too few samples for a rigorous statistical analysis of the data. Supplementary Figs. S1 and S2 show the time series of mean wind direction and wind speed, respectively, associated with each flask sample used in this analysis.

To define isotopic and mole fractions of trace gases in background air, measurements from two additional NOAA-GMD sites were used. For $^{14}CO_2$, CO_2, CO, and CH_4, we used weekly measurements from Niwot Ridge, CO (sitecode NWR, 40.05^o N, 105.63^o W, 3526 m a.s.l.), a site in the alpine tundra with strong westerly winds that only rarely required filtering of samples influenced by pollution from the Denver metro area (Turnbull et al., 2007). For other gases, including acetylene, benzene, and the C_3–C_5 alkanes we used weekly to fortnightly samples collected in the free troposphere from flights at a nearby location (3000 to 4000 m a.s.l. above Briggsdale Colorado; sitecode CAR, 40.37^o N, 104.30^o W, ground elevation ∼1700 m a.s.l.).

2.2 Flask sampling

Discrete whole air samples are collected daily (Andrews et al., 2013) from the BAO tall tower (from an air intake at 300 m) using Programmable Flask Packages (PFPs) connected to a Programmable Compressor Package (PCP) capable of delivering 15 standard L min^{-1}. Each PFP contains 12 cylindrical borosilicate glass flasks (0.7 L each). On each end of the flasks are automated glass-piston stopcocks, sealed with Teflon O-rings. Prior to deployment, each flask in the PFP unit is flushed with clean dry air and then pressurized to ∼140 kPa with synthetic air containing 330 ppm CO_2.

Automated sampling consists of the following steps: (1) a manifold flush, (2) a flask flush, and (4) pressurization of the flask to ∼270 kPa. The entire process takes about 2 min. Sampled air at BAO first passes through a drying stage (dew-point temperature at ambient pressure of ∼5 °C) prior to collection. Sampling is done at midday (19:30 UTC) in most cases; all samples used in this analysis were collected within 30 min of 19:30 UTC. Two flasks are filled within 5 min of each other (∼4 standard liters) which provides enough air for analysis of the standard suite of trace gases (described below), and for analysis of $^{14}CO_2$, which typically requires 0.4 to 0.5 mg C for high precision (<3 ‰) AMS analysis.

2.3 Flask analysis

Each flask pair is analyzed at NOAA–GMD for CO_2, CO, CH_4, SF_6, H_2, N_2O, and a suite of halocarbons and hydrocarbons. Stable isotopes of CO_2 ($\delta^{13}C$ and $\delta^{18}O$) are analyzed at the INSTAAR Stable Isotope Laboratory (Vaughn et al., 2004). In this study, we use measurements of CO_2, CO, CH_4, acetylene (C_2H_2), benzene (C_6H_6), propane (C_3H_8), n-butane (n-C_4H_{10}), n-pentane (n-C_5H_{12}), and i-pentane (i-C_5H_{12}). We also use $\delta^{13}C$ in CO_2 in the calculation of $\Delta^{14}C$, according to methods described by Stuiver and Polach (1977), which is required because the CAMS AMS does not measure the $^{13}C/^{12}C$ ratio on-line.

Dry air mole fractions of CO_2, CH_4, and CO were measured on one of two nearly-identical custom automated analytical systems. These systems consist of custom-made gas inlet systems, calibration systems, gas-specific analyzers, and system-control software. During this project, each system used a different technique to measure CO. One used a Reduction Gas Analyzer, where CO is separated from air by gas chromatography, then passed through a heated bed of HgO producing Hg before it is detected by resonance absorption (Novelli et al., 1998). The second is Vacuum UV Resonance Fluorescence (VURF), where CO is detected by fluorescence at ∼150 nm. Both techniques are calibrated against the same standard scale, and uncertainties (68 % confidence interval) are ∼1 ppb for the VURF and ∼2 ppb for the RGA. Long-term comparison of the two systems shows agreement to within ∼1 ppb. CH_4 was measured by gas chromatography (GC) with flame ionization detection with an uncertainty of ∼1.4 ppb (Dlugokencky et al., 1994). A non-dispersive infrared analyzer is used for CO_2 with an uncertainty <0.1 ppm (Conway et al., 1994).

The non-methane hydrocarbons (C_2H_2, benzene, and C_3–C_5 alkanes) are measured using a gas chromatography-mass spectrometric (GC-MS) technique, with cryogenic preconcentration (Montzka et al., 1993; Miller et al., 2012). Measurement uncertainties for the hydrocarbons considered in this study vary by compound, and include known issues regarding (1) absolute calibration standard preparation errors, (2) the transfer of the absolute scale to the dry compressed whole air reference gases used in routine analyses,

(3) uncertainty in assumed detector sensitivity due to analyte losses during random and sporadic temperature anomalies during the pre-concentration step, and (4) chromatographic baseline interferences (propane only). Storage tests have shown negligible drift in the hydrocarbon mole fractions of reference gases. Therefore, assigned total uncertainties (1σ) are 5 % for n-C_4H_{10}, i-C_5H_{12}, n-C_5H_{12}, and C_6H_6, and 15 % for C_3H_8 due to chromatographic baseline interferences, and 15 % for C_2H_2 due primarily to absolute calibration scale uncertainties. Measurement reproducibility (1σ) is generally <2 % for compounds present at mole fractions >10 ppt. For C_2H_2 and C_3H_8, the most volatile of these compounds, reproducibility was somewhat poorer during these flask analyses due to the instability of the temperature of the cryogenic pre-concentrator (approximately -25 % and $+12$ %). The asymmetric reproducibility is attributed to the different impact that the temperature instability has on quantitation, depending on whether the anomalous temperature occurs during a BAO sample analysis or during analysis of the reference gas. This is primarily a problem only for the higher volatility species, C_2H_2 and C_3H_8. As this temperature instability is a random, sporadic occurrence, we conservatively allow for large negative uncertainties and smaller positive uncertainties in all analyses. An additional bias arising from non-linearity in the GC-MS response to varying analyte concentrations (except for propane, which is marginally linear) is estimated to result in an overestimate in the reported concentrations on the order of 5 % to 12 %. We do not include this bias implicitly in our emission calculations, but we discuss its (minor) impact on our results and conclusions below.

All measurements are reported as dry air mole fractions relative to internally consistent standard scales maintained at NOAA-GMD. We use the following abbreviations for measured dry air mole fractions: ppm = µmol (trace gas) mol (dry air)$^{-1}$, ppb = nmol mol^{-1}, and ppt = pmol mol^{-1}. Additional details on these methods are described at http://www.esrl.noaa.gov/gmd/ccgg/aircraft/analysis.html.

2.4 Radiocarbon analysis

A subset (typically 1 out of every 2 pairs) of the flask pairs are hand selected for analysis of $^{14}CO_2$. The selection is based on a visual inspection of continuous CO and CO_2 observations during the time of sampling. For a typical flask package, 3 pairs (out of the 6 pairs total) are selected for radiocarbon analysis, with two pairs typically having the highest CO and CO_2 concentrations and one pair having CO and CO_2 concentrations closest to background. This approach maximizes the dynamic range of the observations over which tracer/CO_2ff ratios are estimated. Analyses of $^{14}CO_2$ were done by extracting CO_2 from the whole air samples using cryogenic separation, reducing the extracted CO_2 to graphite, and atom counting via accelerator mass spectrometry (AMS). Extractions of authentic samples, measurement controls, and process blanks were performed at the University of Colorado INSTAAR Laboratory for AMS Radiocarbon Preparation and Research (NSRL) using an automated extraction system (Turnbull et al., 2010). Graphitization and AMS analysis was done at LLNL-CAMS. A description of the high precision methods for analysis of atmospheric samples at CAMS is given by Graven et al. (2007). The measurements are expressed as age-corrected $\Delta^{14}CO_2$ in units of per mil (‰), calculated from the $^{14}C/^{13}C$ ratio (normalized to a $\delta^{13}C$ of -25‰), measured relative to NBS Oxalic Acid I (OX1), and reported relative to the absolute radiocarbon standard, as detailed in Stuiver and Polach (1977). It should be noted that our use of $\Delta^{14}CO_2$, is equivalent to the use of Δ in Stuiver and Polach.

Uncertainty in these observations is assigned as the standard deviation (1σ) of a series of repeat measurements on extraction aliquots of whole air stored in high pressure cylinders. Air from two surveillance cylinders having different but near-ambient ^{14}C activities, identified as NWT3 and NWT4, were extracted, graphitized, and analyzed concurrent with the BAO samples across 7 different measurement "wheels" or batches. Multiple samples of NBS Oxalic Acid II (OX2, a commonly used secondary standard) were combusted, graphitized and analyzed simultaneously. Typically, in a wheel containing 25 authentic samples, 12 measurement controls and 1 process blank were analyzed. For the observations described in this study, the (1σ) repeatability (standard deviation) of NWT3 and NWT4 samples was ±2.2‰ ($n = 140$). AMS measurement uncertainty (based on counting statistics) typically contributes about 1.3–1.7‰ of the total uncertainty. In a small number of cases, the internal variability on the measurement of an unknown sample was larger than the repeatability of the pool of NWT samples. The larger of the two is assigned as the uncertainty for a given $\Delta^{14}CO_2$ measurement.

2.5 Calculation of CO_2ff

Recently added fossil fuel CO_2 (CO_2ff) is defined as the local enhancement of CO_2, with respect to an appropriate background reference site, due to fossil fuel emissions. CO_2ff is estimated using a mass balance approach (Levin et al., 2003), in which the observed mole fraction of CO_2 (CO_2obs) is partitioned into background CO_2 (CO_2bkg), fossil CO_2, and biogenic CO_2 (CO_2bio) components. CO_2bio is the net balance between respired CO_2 (CO_2resp) and CO_2 taken up by photosynthesis (CO_2photo). We further separate the respired fraction into autotrophic respiration (CO_2auto) and heterotrophic respiration (CO_2het) that originates from older soil carbon pools (which typically contain more bomb ^{14}C). Equations (1a) and (1b) detail this mass balance relationship, as formulated in Turnbull et al. (2006), with CO_2resp separated into heterotrophic and autotrophic components. Similarly, an isotopic mass balance equation (Eq. 2) can describe the contribution of these three end members to the total

observed $\Delta^{14}C$.

$$CO_2obs = CO_2bkg + CO_2ff + CO_2bio \quad (1a)$$

$$CO_2bio = CO_2auto + CO_2het - CO_2photo \quad (1b)$$

$$\Delta^{14}_{obs}CO_2obs = \Delta^{14}_{bkg}CO_2bkg + \Delta^{14}_{ff}CO_2ff + \Delta^{14}_{bio}CO_2bio \quad (2)$$

Since $\Delta^{14}C$ values are all normalized by their $\delta^{13}C$ values, and thus are not influenced by natural fractionation, we can assume that Δ^{14}_{photo} and Δ^{14}_{auto} are identical to Δ^{14}_{bkg} (Turnbull et al., 2006). The system of equations can then be solved for CO_2ff to give Eq. (3).

$$CO_2ff = \left(\frac{CO_2obs(\Delta^{14}_{obs} - \Delta^{14}_{bkg})}{(\Delta^{14}_{ff} - \Delta^{14}_{bkg})}\right) - \left(\frac{CO_2het(\Delta^{14}_{het} - \Delta^{14}_{bkg})}{(\Delta^{14}_{ff} - \Delta^{14}_{bkg})}\right) \quad (3)$$

In this equation, the variables in the first term are either known ($\Delta^{14}_{ff} = -1000‰$) or can be measured. We use observations from NWR to estimate Δ^{14}_{bkg}. The background is estimated by applying a smoothing algorithm (Thoning et al., 1989) to the NWR data (a curve-fit of 3 polynomials, 4 harmonics, and added low-pass filtered residuals), after filtering out samples influenced by upslope flows carrying locally influenced air, characterized by high CO/CO_2 ratios, as in Turnbull et al. (2007). Smoothed NWR results used here are from Lehman et al. (2013). The standard deviation of the residuals from the smoothing fit are calculated to be 1.7‰ . The selection of a proper background site is thought to introduce uncertainties on the order of the measurement uncertainty (∼2‰) (Turnbull et al., 2009). We define the uncertainty in CO_2ff as 1.2 ppm, estimated from the measurement uncertainty in Δ^{14}_{bkg} and Δ^{14}_{obs} (± 2.2‰).

The second term in Eq. (3) is a minor correction to the calculation of CO_2ff due to heterotrophic respiration from soils, which can draw from carbon pools that are on the order of tens of years old, and thus reflect the higher $\Delta^{14}CO_2$ in the atmosphere at the time. The magnitude of this correction can be estimated from a terrestrial ecosystem model, such as the CASA biogeochemical model (Thompson and Randerson, 1999); we follow the estimates of Turnbull et al. (2009) for North American mid-latitudes and set this correction to −0.2 (± 0.1) ppm (thus resulting in a positive offset) from October to March and to −0.5 (± 0.3) ppm from April to September. Since the correction term in Eq. (3) is subtracted from the first term, the impact of heterotrophic respiration is to raise estimates of CO_2ff in both seasons.

The influence of additional sources on $\Delta^{14}obs$ is globally variable and has potential contributions from stratospheric intrusion of cosmogenically produced and bomb-era ^{14}C (e.g. Levin et al., 2010; Graven et al., 2012a), nuclear reactors (e.g. Graven and Gruber, 2011), biomass burning (e.g. Schuur et al., 2003; Vay et al., 2011), and the oceanic-atmosphere disequilibrium (e.g. Sweeney et al., 2007; Muller et al., 2008). However, model-based estimates of the $\Delta^{14}C$ signal (not including those from nuclear emissions) in the conterminous United States (Miller et al., 2012) show that these terms contribute very little relative to the spatial gradients arising from fossil fuel combustion. Graven and Gruber (2011) argue that in the eastern United States nuclear contributions may be significant, but they predict near-zero nuclear influence in most of the western United States, including Colorado. Any contribution from stratosphere or ocean sources at BAO is likely to simultaneously impact the NWR background site and, thus, can be ignored in this analysis. At least one sample was influenced by a biomass burning event, identified by an anomalously high CO/CO_2ff ratio, as well as multiple news reports of poor air quality on that particular day resulting from the Station Fire in southern California in August 2009 (e.g. Brennan, 2009). This sample, along with one other that exhibits an abnormally high CO/CO_2ff ratio is omitted from this analysis. The sample influenced by the wildfire plume was collected 1 September 2009; the other sample, collected 30 January 2010, is unusual in that the estimated CO_2bio mole fraction (calculated as CO_2obs – CO_2ff–CO_2bkg) was very large (15 ppm), and about twice the estimated CO_2ff for this sample. The large CO_2bio relative to other samples in the dataset suggests the possibility of an undetected stratospheric or biomass burning influence or an unusually large heterotrophic respiration signal. We therefore exclude this point (30 January 2010 sample) from our analysis. In addition to CO, a large number of other anthropogenic tracers were elevated in this particular sample, suggesting that stratospheric influence is, in the end, not likely.

2.6 Estimating tracer/CO_2ff enhancement ratios

Tracer/CO_2ff enhancement ratios are calculated by taking the median of individual tracer/CO_2ff ratios after subtracting the background from each trace gas. The median ratios derived from individual samples provides a more robust estimate of the apparent tracer/CO_2ff ratios than that determined from either a linear regression slope or an arithmetic mean, which may give estimates that are overly sensitive to ratio outliers that can result from signals due to air masses in which emissions of various sources are not well mixed (Miller et al., 2012). While the linear regression method has the advantage of being less sensitive to the selection of background site, when considering observations across seasonal to annual time scales a seasonally varying background may still bias the slope determination. Since the BAO tower and the NWR and CAR background sites are closely situated, it is likely that any background-related biases are small. The tracer/CO_2ff ratios are shown in Table 1. For comparison, estimates of slopes are also provided in Table 1 for each tracer/CO_2ff pair, derived using a two-way least squares regression algorithm which estimates the geometric mean of the X-Y and Y-X regressions (without forcing the intercept through zero). Significant differences exist between the slopes and median ratios for many of the tracers, in particular for those with lower coefficients of determination

Table 1. Summary of observed tracer/CO_2ff ratios and associated uncertainties. Ratios estimated using the median point-by-point calculation as well as from a two way linear regression. Correlation coefficients (r^2) are also provided. For the C_4 and C_5 alkanes, C_2H_2, and benzene, a nonlinearity bias in the GC-MS response results in an estimated 5–12 % overestimate in the tracer/CO_2ff ratios for these gases.

Species	Wind Sector	n	Ratio (units)		Ratio confidence limits (2σ)		n	Slope (units)		Slope confidence limits (2σ)		r^2
					min	max				min	max	
CO	N/E	43	8.8	(ppb ppm^{-1})	7.3	9.4	55	8.5	(ppb ppm^{-1})	7.1	10.5	0.70
	S	22	10.5	(ppb ppm^{-1})	7.3	13.8	31	7.2	(ppb ppm^{-1})	5.7	9.6	0.89
	Combined	65	9.0	(ppb ppm^{-1})	8.1	9.8	86	7.8	(ppb ppm^{-1})	6.5	9.3	0.83
CH_4	N/E	43	31.3	(ppb ppm^{-1})	24.3	34.9	55	30.7	(ppb ppm^{-1})	22.1	34.5	0.81
	S	23	9.5	(ppb ppm^{-1})	5.8	12.4	33	8.1	(ppb ppm^{-1})	5.0	11.4	0.75
C_2H_2	N/E	41	44.5	(ppt ppm^{-1})	39.8	52.5	53	63.6	(ppt ppm^{-1})	37.6	73.5	0.81
	S	22	44.9	(ppt ppm^{-1})	34.7	61.6	32	45.2	(ppt ppm^{-1})	36.8	62.5	0.78
	Combined	63	44.5	(ppt ppm^{-1})	40.7	51.8	85	52.1	(ppt ppm^{-1})	40.4	65.6	0.79
BENZ	N/E	41	29.0	(ppt ppm^{-1})	22.2	36.5	53	33.7	(ppt ppm^{-1})	21.9	38.7	0.81
	S	22	19.8	(ppt ppm^{-1})	14.8	26.2	32	14.2	(ppt ppm^{-1})	10.7	19.8	0.72
iC_5H_{12}	N/E	41	277.5	(ppt ppm^{-1})	243.1	395.9	53	485.2	(ppt ppm^{-1})	297.9	565.1	0.75
	S	21	88.1	(ppt ppm^{-1})	47.6	120.7	31	65.4	(ppt ppm^{-1})	51.6	100.7	0.80
nC_5H_{12}	N/E	41	314.1	(ppt ppm^{-1})	236.8	402.4	53	480.6	(ppt ppm^{-1})	318.9	566.8	0.74
	S	21	70.4	(ppt ppm^{-1})	37.4	106.0	31	54.5	(ppt ppm^{-1})	40.1	86.1	0.78
nC_4H_{10}	N/E	41	899.3	(ppt ppm^{-1})	707.9	1248.0	53	1520.8	(ppt ppm^{-1})	950.3	2085.1	0.71
	S	21	193.3	(ppt ppm^{-1})	104.8	251.3	31	152.3	(ppt ppm^{-1})	102.6	212.8	0.75
C_3H_8	N/E	41	2035.2	(ppt ppm^{-1})	1615.8	2989.2	52	3265.1	(ppt ppm^{-1})	2048.4	4979.5	0.51
	S	21	449.1	(ppt ppm^{-1})	243.3	612.1	31	352.7	(ppt ppm^{-1})	198.0	539.0	0.61

(r^2). Samples are only used in the median ratio calculation when the estimated CO_2ff is above the 1.2 ppm 1σ detection limit to remove divide-by-zero errors, while no lower limit is used in the slope calculations. Removing this filter impacts the uncertainties of the median ratios (by up to ∼50 %), but it has a smaller impact on the median ratios themselves, typically impacting the tracer/CO_2ff ratios by less than ± 10 %, except for the C_3–C_5 alkanes in the S wind sector which are impacted by between +15 and +30 %. In general, the application of this filter increases the enhancement ratios in the S wind sector and reduces them in the N/E wind sector. The supplementary material accompanying this manuscript includes figures (Figs. S3–S10) showing the data used to derive the median ratios, including time series and histograms of the dataset both with and without the wind speed and low CO_2ff cut-off filters.

Uncertainties in the median ratios are 95 % confidence intervals, defined as the 2.5–97.5 percentile range (∼2σ confidence) from a distribution of 500 estimates of the median from a randomized re-sampling of the data (boot-strapping with replacement). We also estimated the uncertainty in the tracer/CO_2ff enhancement ratios associated with measurement uncertainty (both for the trace gas and CO_2ff) and found that these uncertainties (at 2σ) were comparable to or lower than the boot-strap approach in all cases. For C_2H_2, $n-C_4H_{10}$, $n-C_5H_{12}$, $i-C_5H_{12}$, and C_6H_6, the nonlinearity in the GC-MS response results, potentially, in an additional overestimate in the tracer/CO_2ff ratios for these gases of as much as 5–12 %. This bias has yet to be fully evaluated for each gas, and is therefore not incorporated into the reported enhancement ratios.

A measure of the appropriateness of the tracer/CO_2ff approach for deriving apparent emission ratios is estimated by calculating the r^2 from a linear regression of tracers vs. CO_2ff; a high r^2 suggests that emissions of the tracers are appreciably co-located with fossil fuel combustion sources. Results from the tracer/CO_2ff enhancement ratio calculations (with associated uncertainties, slopes, and r^2 values) are detailed in Table 1. Background observations for the different trace gases are taken from one of two nearby sites in the NOAA-GMD global network, either NWR (CO and CH_4) or from flights at CAR (acetylene, benzene, and the C_3–C_5 alkanes). CO and CH_4 observations are available from both sites and we confirmed that the enhancement ratio estimates are not appreciably sensitive to the selection of background site (differences between 7 % and 15 % in derived enhancement ratios).

The sensitivity of this analysis to the prescribed heterotrophic respiration correction to CO_2ff (Eq. 3) was determined by recalculating the tracer/CO_2ff ratios with this correction term doubled, in one case, and set to zero in another. The ratios estimated from this sensitivity test were within the 95 % confidence intervals in all but two cases (CO and C_2H_2), where the recalculated estimates were outside of the confidence intervals only by a few percent. Thus, we consider the uncertainty in the heterotrophic respiration correction to CO_2ff to be a largely insignificant source of error in our analysis. Given the relative lack of vegetation in the region

Table 2. Summary of trace gas lifetimes and major emission sources influencing observations at BAO (Watson et al., 2001; Pétron et al., 2012).

Species	Atmospheric Lifetime[a]	Major sources near BAO
carbon monoxide (CO)	49 days	on-road and non-road gasoline combustion
methane (CH_4)	6.9 yr	oil and gas systems[b], waste water treatment, landfills, cattle feed lots
acetylene (C_2H_2)	17 days	mobile sources (combustion)
benzene (C_6H_6)	10 days	mobile sources (combustion and evaporative), oil and gas systems
iso-pentane ($i-C_5H_{12}$)	3.0 days	mobile sources (combustion and evaporative), oil and gas systems
n-pentane ($n-C_5H_{12}$)	3.1 days	oil and gas systems, mobile sources (combustion and evaporative)
n-butane ($n-C_4H_{10}$)	4.9 days	oil and gas systems
propane (C_3H_8)	12 days	oil and gas systems
CO_2ff[c]	N/A	on-road vehicles (33%), electricity prod. (32 %), residential (11 %), airborne (10 %), other (14 %)

[a] Atmospheric lifetimes estimated for $[OH] = 1 \times 10^6\ cm^{-3}$ using published rate constant data (Atkinson et al., 2006; NASA, 2006).
[b] Sources include condensate tanks, well drilling and completion, distribution systems, refineries. [c] Source distribution according to Vulcan v2.2 for Weld/Larimer and Denver metro counties in 2008.

surrounding BAO, it is more likely that the prescribed respiration correction is biased high rather than low, which would result in CO_2ff values that are biased high and tracer/CO_2ff enhancement ratios that are biased low.

2.7 Bottom-up fossil fuel CO_2 emissions estimates

To derive top-down emissions estimates for the observed trace gases via tracer/CO_2ff enhancement ratios, we use both county-level and gridded bottom-up fossil fuel CO_2 emissions estimates from the Vulcan data product (v2.2) (Gurney et al., 2009) as a quantitative reference. Vulcan (http://vulcan.project.asu.edu) is a high resolution data product that utilizes a combination of energy, air quality, census, traffic, and digital road statistics to quantify fossil fuel CO_2 emissions for the United States. Until recently, the Vulcan inventory was available only for 2002, but is now updated to include annual emissions at the county and state level for all years between 1999 and 2008. The gridded high resolution product is currently available only for 2002, however. The Vulcan02 data product is used as the base year in this analysis. For the Vulcan02 product, country-wide emissions are in agreement with the United States Energy Information Administration (EIA) estimates to about 2 % even though the different estimates were compiled using independent statistical datasets (Gurney et al., 2011). At the county level, the estimated uncertainty (1σ) on annual CO_2ff emissions from the Vulcan02 data product is variable, but no more than $\sim$20 % (and typically less than $\sim$10 %) for any given county (Gurney et al., 2011). To apply the Vulcan02 data product to our analysis period (2009–2010), the Vulcan02 emissions are scaled up to the observation period using the state-level EIA inventory (EIA, 2012), which is currently available through 2009. We use the county-level Vulcan data product for 2003–2008 to constrain the uncertainty in our scaling factor derived from the state-level EIA data. A more detailed description of the scaling procedure and associated uncertainty is provided below (Sect. 3.3).

Vulcan emission rates for CO_2 are given in Table 3 for two source regions that correspond to the N/E and S wind sectors, as defined above (Sect. 2.6). For simplicity we define the N/E wind sector as being influenced primarily by emissions from Weld and Larimer Counties and the S wind sector as being influenced primarily by emissions from Adams, Broomfield, Arapahoe, Jefferson, and Denver Counties (collectively referred to here as the Denver metro counties). Total CO_2ff emissions, according to Vulcan02, are estimated to be 2.94 Tg C and 7.27 Tg C for the N/E (Weld and Larimer Counties) and S (Denver metro counties) wind sectors, respectively. The on-road, electrical production, residential, and airborne sectors contribute to 86 % of the total CO_2ff emissions in the region (Table 2). In Sect. 3.3.1, we consider the uncertainties associated with these assumptions about the geographic area influencing emissions in the two wind sectors.

2.8 Bottom-up trace gas emissions estimates

We compare our top-down emission estimates with bottom-up estimates for CO (NEI, 2008) and acetylene (NEI, 2005). Emissions of C_2H_2 are estimated from a gridded NEI05 inventory of total VOC emissions in combination with the EPA SPECIATE(v4.3) model (EPA, 2011).

Table 3 summarizes the bottom-up emission estimates, including the base-year for each inventory. Scaling factors (α) for the trace gases that relate the inventory base-year to the observation period are estimated from population statistics or additional factors. Scaling of the tracer inventories, which are related primarily to mobile emissions, is calculated in proportion to the rate of increase in population according to statistics from the US Census Bureau. The uncertainty limits for the scaled emissions are assigned as the base year estimates (i.e. no change in emissions) on the low end to an

Table 3. Summary of top-down and bottom-up annual emissions for CO and C_2H_2, including the bottom-up emission source, inventory base year, the scaling term (α), and associated uncertainties derived for different regions around the sampling site in Colorado for the measurement period. Bottom-up emissions for CO_2ff are also summarized. Uncertainties on the scaled bottom-up emissions and the top-down emissions are described in Sects. 3.3 and 3.3.1.

Species	Wind Sector	Bottom-Up Emissions		Source	Base Year	α (%)	α min/max		Scaled Emissions		Scaled Emissions Min/Max		Top-Down Emissions (E_x)		E_x Min/Max	
							min	max			min	max			min	max
CO	N/E	116.0	Gg	NEI08	2008	3.6	−10.5	11	120.1	Gg	103.8	128.4	62.4	Gg	46.0	75.5
	S	362.1	Gg	NEI08	2008	1.7	−10.5	5	368.2	Gg	324.1	380.5	182.5	Gg	116.8	251.2
	Combined	478.1	Gg	NEI08	2008	–	–	–	488.3	Gg	427.9	508.9	221.1	Gg	171.0	269.5
C_2H_2	N/E	0.172	Gg	NEI05	2005	11.6	0	35	0.192	Gg	0.172	0.232	0.291	Gg	0.225	0.369
	S	0.544	Gg	NEI05	2005	5.2	0	16	0.572	Gg	0.544	0.629	0.727	Gg	0.506	1.034
	Combined	0.643	Gg	NEI05	2005	–	–	–	0.764	Gg	0.716	0.861	1.011	Gg	0.791	1.273
CO_2	N/E	2.94	Tg C	Vulcan2.2	2002	2.8	–	–	3.02	Tg C	2.42	3.63	–	–	–	–
	S	7.27	Tg C	Vulcan2.2	2002	2.8	–	–	7.47	Tg C	5.98	8.97	–	–	–	–

estimate using a scaling factor that is 3 times the population increase on the high end. An exception to this is for the uncertainty limits for CO emissions. There is evidence that on-road mobile CO emissions have decreased in many urban regions over the past 15–20 yr despite large population increases, and in Denver, specifically, the CO-to-fuel burnt ratio was observed to have decreased at a rate of about 7 % per year between 1999 and 2007 (Bishop and Stedman, 2008). Therefore, the bottom-up CO emissions uncertainty is bracketed at the low end by an emission rate corresponding to a decrease in emissions of 10.5 % from 2008 (the inventory base year) to the observation period. We acknowledge that scaling up of these trace gas estimates using population statistics is an unconstrained approximation, and we have, therefore, assigned conservatively large uncertainties. It is important to note, however, that the inventory base year estimate is always within the uncertainty brackets of the scaled inventory values, thus allowing the reader to evaluate the top-down and bottom-up comparison independent of any scaling assumptions made here.

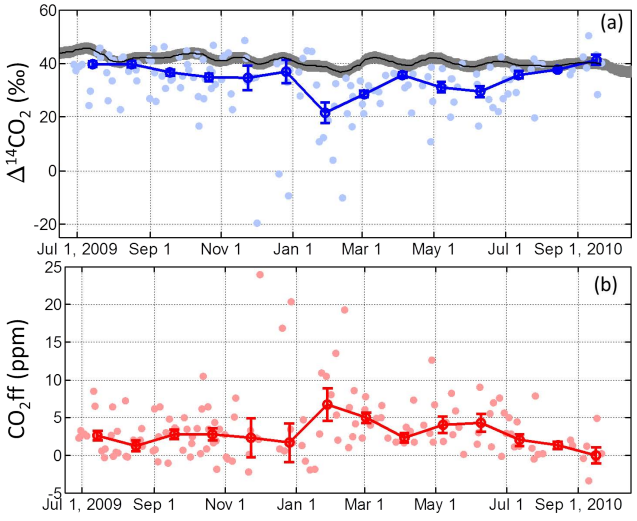

Fig. 2. Time series of $^{14}CO_2$ **(a)** and CO_2ff **(b)** from 145 discrete whole air samples (filled circles) collected at the BAO tower. Uncertainty in each $^{14}CO_2$ measurement is ± 2.2‰, which translates to an uncertainty in each CO2ff observation of 1.2 ppm (see Sect. 3.1). Thirty day binned medians are shown as open circles in both **(a)** and **(b)**, with error bars representing the standard error of the mean (1σ) for each 30 day bin. Also shown in **(a)** is the $^{14}CO_2$ background as observed at NWR (black line) (Turnbull et al., 2007; Lehman et al.,2013), with the uncertainty envelope represented by the grey shaded region.

3 Results and discussion

3.1 $\Delta^{14}C$ and CO_2ff time series

The results of the $^{14}CO_2$ analyses are shown in Fig. 2a with values ranging from −19.4 to 50.5‰. The time series runs from late June 2009 to September 2010, overlapping with the observation period of the CFRPS, where observations (from the same set of flask samples) up through the spring of 2010 were included in their top-down emission calculations. Excursions of $\Delta^{14}CO_2$ at BAO (relative to the NWR background site) towards lower values signify the addition of recently emitted fossil fuel CO_2 to the sampled air mass. As described in Sect. 2.5, the CO_2ff mole fraction can be quantified using Eq. (3), with an uncertainty of 1.2 ppm based on propagation of the analytical uncertainty in $\Delta^{14}CO_2$ for both Δ^{14}obs and Δ^{14}bkg (the uncertainty in CO_2 terms is small relative to those for $\Delta^{14}C$). Performing this calculation for each BAO observation in Fig. 2a gives CO_2ff mole fractions that range from below the 1.2 ppm detection limit up to 25 ppm. There are occasional instances of negative CO_2ff values (14 % of all samples), which is not physically realistic. All but 5 of these samples (3 % of the entire dataset) lie within the 1σ envelope around zero and only 1 sample (−3.3 ppm) lies outside of 2σ, thus these negative values are statistically consistent with $CO_2\text{ff} = 0 \pm 1.2$ ppm.

The most obvious feature of the CO_2ff variability is that mole fractions are high and variable in the winter months and

relatively constant and lower, on average, during the summer months (Fig. 2b). This trend is qualitatively consistent with shallow, and variable, mixing layer heights in the winter and deep mixing layers in the summer (Turnbull et al., 2009). Mixing layer height is driven by a number of complex meteorological and topographical variables, but largely by surface sensible heat flux, which is of course much lower during the winter. Tracer/tracer ratios are expected to be much less sensitive to variability in mixing layer height since the dilution and mixing of co-located and temporally co-varying emissions will impact the different tracers equally. As we describe below, observations of a set of tracer/CO_2ff ratios are consistent with this expectation.

3.2 Variability in tracer/CO_2 ff enhancement ratios

When sources of trace gas emissions are co-located with fossil fuel combustion sources, an analysis of the trace gas enhancements relative to CO_2ff provides a means to better understand the variability in the mix of emission sources influencing the site independent of the dilution and mixing dynamics that impact absolute mole fractions. While variability in the absolute mole fractions of CO_2ff has a strong seasonal dependence (Fig. 2b), with larger enhancements observed in the winter than the summer, there is no apparent (statistically significant) seasonality to any of the considered tracer/CO_2ff enhancement ratios, suggesting that boundary layer dynamics are largely what are driving the seasonality in measured atmospheric mole fractions or that emissions of all the trace gases have similar seasonal cycles to CO_2ff.

Figure 3a and b show the dependence of the CO/CO_2ff and CH_4/CO_2ff enhancement ratios on wind direction using two different size wind direction bins (40° and 135°), demonstrating a significant enhancement in CH_4 abundance (relative to CO_2ff) when winds are arriving from the north and east of the BAO tower. The CO/CO_2ff ratio, on the other hand, is relatively constant with wind direction such that the uncertainties in the different sectors overlap, suggesting a consistent mix of CO and CO_2ff combustion sources throughout the region. The CH_4/CO_2ff variability with wind direction shows two distinct wind sectors within which the CH_4/CO_2ff ratio is relatively stable. A significant drop-off in the CH_4/CO_2ff ratio can be seen at around $\geq$ 115–120°, which corresponds to sectors having fewer oil and gas wells and stronger influence from the Denver metropolitan region. This provides the basis for the definition of the N/E and S wind sector boundaries, which we use to examine differences in emissions for each trace gas considered in the analysis that follows.

The variability in CH_4/CO_2ff with wind direction is consistent with results presented in the CFRPS (Pétron et al., 2012), which found significantly enhanced mole fractions of alkanes, including CH_4, C_3H_8, n-C_4H_{10}, $i-C_5H_{12}$, and n-C_5H_{12}, observed at BAO in air masses arriving from the N/E. Benzene was also enhanced in air masses arriving from the

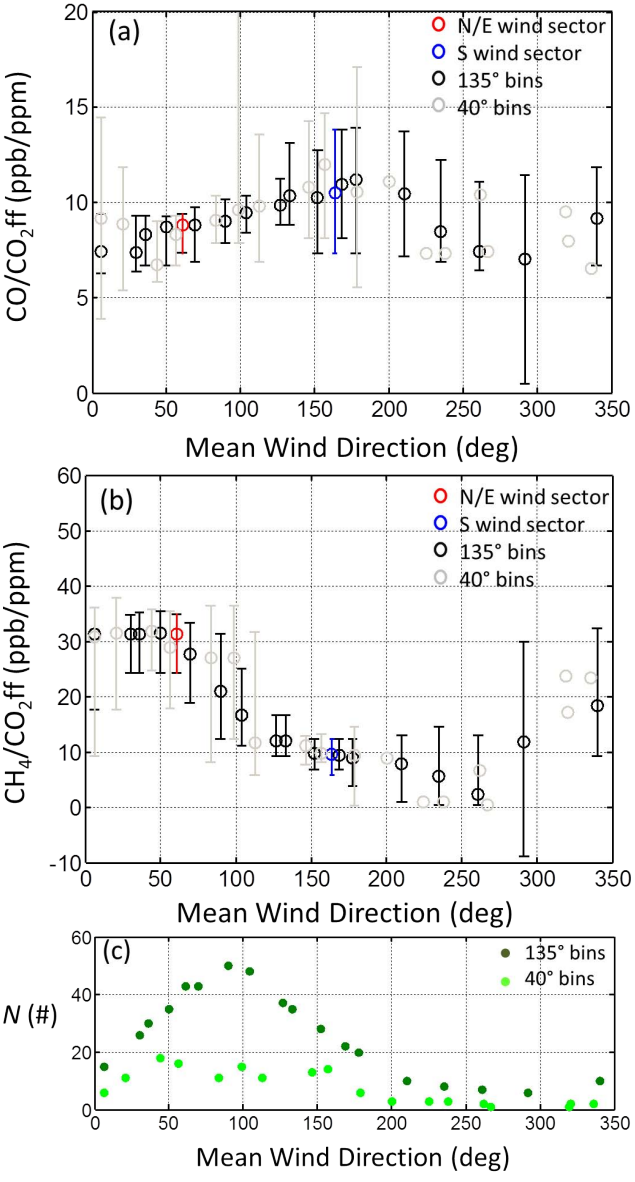

Fig. 3. Tracer/CO_2ff ratios as a function of mean wind direction for **(a)** CO and **(b)** CH_4 for each rotating 135°-wide and 40°-wide wind sector wedge. The number of observations in each 135° and 40° wedge is shown in **(c)**. Also shown are the tracer/CO_2ff ratios calculated for the N/E (red) and S (blue) wind sectors used in the analysis.

N/E. These differences were attributed to oil and gas production in Weld County, to the northeast of BAO. As shown on the map in Fig. 1, the majority of these wells are located in Weld County (COGCC, 2011), from which 17.9 million barrels of oil and 5.7 billion cubic meters of natural gas were produced in 2009 (COGCC, 2011). Other sources of CH_4 in this region include cattle feedlots, landfills, waste water treatment plants, and natural gas processing plants. The transportation or mobile sector contributes significantly to a

subset of the gases considered: CO, C_2H_2, C_6H_6, $i-C_5H_{12}$, and, to a lesser extent, $n-C_5H_{12}$ (Watson et al., 2001). This sector likely contributes significantly to emissions from the Denver metro counties, but there are also significant mobile emissions in the N/E wind sector from Interstate 25, the main north-south route in Colorado, as well as in a number of population centers, including Fort Collins, all located due north of BAO, in Larimer County. Table 2 summarizes the expected sources of the trace gases evaluated in this analysis, along with their expected atmospheric lifetime with respect to oxidation by OH. Lifetimes of the tracers considered range from 3 days (pentanes) to 7 yr (CH_4) (calculated with a constant OH density of 10^6 cm^{-3}). The oxidation of tracers can potentially reduce the observed enhancement ratio, lowering the apparent emission ratio. However, with no statistically significant seasonal differences for any of the tracer/CO_2ff ratios, we see no evidence of strongly seasonal OH chemistry impacting the tracer/CO_2ff ratios discussed here. This is likely a result of short transit times since emission relative to their atmospheric lifetimes.

3.2.1 Carbon monoxide

Figure 4a shows the relationship between CO enhancement and CO_2ff for each sample. Fits of a linear regression are included in the Fig. 4a for the N/E and S wind sectors, giving r^2 values of 0.70 ($n = 55$) and 0.89 ($n = 31$), respectively. As detailed in Table 1, the point-by-point analysis of these observations show median (with 2σ equivalent confidence intervals) CO/CO_2ff enhancement ratios of 8.8 (7.3–9.4) and 10.5 (7.3–13.8) for the N/E and S wind directions, respectively. For all wind sectors combined, the median ratio is 9.0 (8.1–9.8) ($r^2 = 0.83$).

A comparison of these CO/CO_2ff ratios with those found in other studies and those predicted by bottom-up inventories are shown in Fig. 5. The observed ratios from both wind sectors are similar to the values of 6.8 ± 2.2 and 11.7 ± 5.5 ppb ppm^{-1} calculated at Niwot Ridge from two samples originating from the Boulder area via upslope winds in 2004 (Turnbull et al., 2006). Our estimates are somewhat lower, however, than previous reported values of CO/CO_2ff in Denver, where ratios were derived from linear correlations across 4 different aircraft flights (~4-6 samples per flight) in May and July of 2004 (Graven et al., 2009). The observed ratios from these flights ranged from 14–27 ppb ppm^{-1}. Reductions in CO emissions from mobile sources between 2004 and 2009 are well documented (e.g. Bishop and Stedman, 2008) (part of a much longer term trend across most of the country), and could be a factor in the lower enhancement ratios observed here. The long term dataset from BAO, however, provides a more robust estimate of the CO/CO_2ff ratio than either of these short-term studies where small errors in individual data points could result in a large difference in the estimated ratio and where short term variability could have a strong influence. For comparison with these short term datasets, observed ratios of CO/CO_2ff for individual samples from the south wind sector at BAO range from 3.6 to 13.5 ppb ppm^{-1} (1σ), with a maximum observed value of 20 ppb ppm^{-1} (not including the sample impacted by biomass burning). Differences in the influencing area of emissions between the two studies may also play a role in the observed differences.

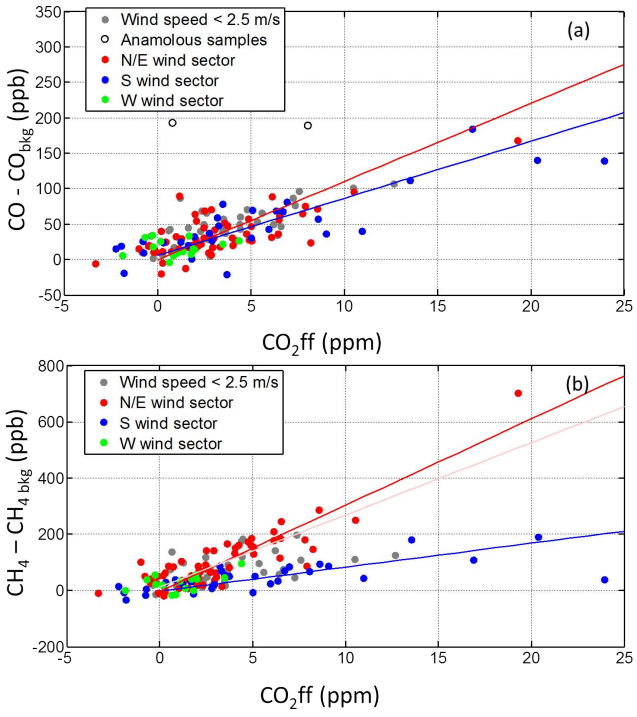

Fig. 4. Correlation plots of CO **(a)** and CH_4 **(b)** enhancements (with respect to background observations) with CO_2ff. Data are separated into three wind sectors (north and east: red; south: blue; and west: green), except in cases where average wind speeds were below 2.5 m s^{-1} over the 30 min prior to sampling. Best-fit lines are shown for the N/E and S wind sectors (correlation coefficients are given in Table 1). In **(a)**, two points are shown as open circles which are omitted from our analysis (see Sect. 2.5). In **(b)**, a second best-fit line (light red) is shown for the N/E data, but excludes the highest CO_2ff sample.

The main anthropogenic sources of CO in Colorado, and in much of the US, are from on-road gasoline vehicles in the mobile sector (66 %) and from non-road gasoline-based equipment (26 %) (NEI, 2008). While the on-road and non-road sectors account for 92 % of total CO emissions in Colorado, these sectors contribute only 29 % of the total state CO_2ff emissions according to the Vulcan08 data product (Gurney et al., 2009). Therefore, the remaining 71 % of CO_2ff sources contributes to at most 8 % of the total CO NEI emissions estimate in Colorado. This suggests that the average CO/CO_2ff emission ratio across a given region is expected to scale roughly with the fraction of CO_2ff emissions coming from on-road and non-road combustion sources.

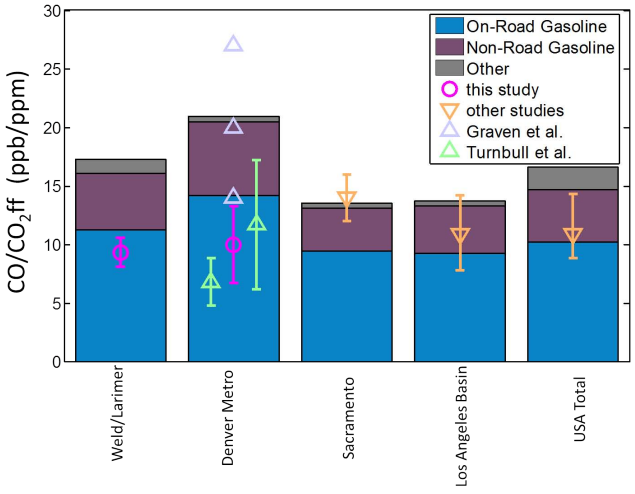

Fig. 5. A comparison of CO/CO_2ff ratios observed or estimated in various US locations. The bars are calculated from bottom-up emissions estimates (NEI08 CO and Vulcan2.2 CO_2) and color-coded by the contribution of different sectors to the total CO emissions: on-road gasoline, non-road gasoline, and other. Observations from each location are shown, including those from our observations at BAO (split into Weld/Larimer and Denver metro influence based on wind sector) and observations from other studies: Denver (Turnbull et al., 2006; Graven et al., 2009)), Sacramento (Turnbull et al., 2011), LA Basin (which includes Los Angeles, Riverside, Orange, and San Bernardino counties) (Djuricin et al., 2010), and for the northeastern US (Miller et al., 2012).

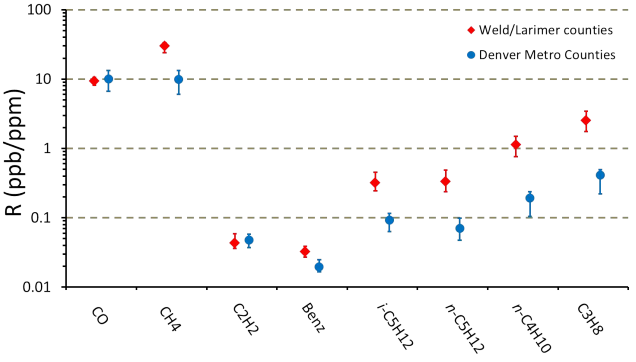

Fig. 6. Observed tracer/CO_2ff ratios from Weld County (N/E wind sector, red diamonds) and the Denver metro counties (S wind sector, blue circles). Ratios are calculated as the median of the point-by-point ratios for all data where CO_2ff was detected above 1.2 ppm, as described in Sect. 3.3. Uncertainties in the median ratios are the 95 % confidence intervals, defined as the 2.5–97.5 percentile range ($\sim 2\sigma$ confidence) from a distribution of 500 median estimates from a randomized re-sampling of the data (boot-strapping with replacement). Note that the figure is presented using a logarithmic scale.

Similar observed CO/CO_2ff ratios for both N/E and S wind sectors, therefore, suggests a similar contribution of on-road and non-road CO_2ff sources in both Weld/Larimer counties and the Denver metro counties, consistent with the Vulcan data product which estimates that the on-road plus non-road sectors (the dominant CO contributors) combine for 29 % and 41 % of the total CO_2 emissions, for Weld/Larimer and Denver metro area respectively (Gurney et al., 2009). This is in contrast to CH_4 and other trace gases, as we discuss below, where there is a clear enhancement due to non-combustion sources related to oil and gas production in the N/E sector.

3.2.2 Methane

We find significant differences in the mole fraction enhancement of CH_4 relative to CO_2ff depending on wind direction (Fig. 4b). The ratio in air arriving from the N/E sector is 31.3 (24.3–34.9) ppb ppm^{-1} and that for air traveling from the S wind sector is 9.5 (5.8–12.4) ppb ppm^{-1}. This higher enhancement ratio in the N/E wind sector can also be visualized in the correlation plot of CH_4 enhancement with CO_2ff (Fig. 4b), where filtering by wind sector results in two highly correlated relationships with different slopes. An r^2 of 0.81 ($n = 55$) and 0.75 ($n = 33$) is calculated for the N/E and S wind sectors, respectively. The high correlation in the N/E wind sector is influenced by the sample at relatively high CO_2ff ($\sim$19 ppm CO_2ff); removing this single data point reduces the r^2 to 0.65, but has little to no impact on the median enhancement ratio (30.2 (22.6–34.9) ppb ppm^{-1}). The median enhancement ratio is higher by a factor of 3 in the N/E wind sector relative to the S wind sector, implying that emissions of CH_4, relative to CO_2ff, are 3 times higher in the N/E sector than the S sector. The added source of CH_4 influencing air samples arriving from the N/E likely results from a mix of emissions from oil and gas operations in the DJB (Pétron et al., 2012), and other non oil and gas sources, such as cattle feedlots.

Entrained CO_2ff can be co-emitted from natural gas wells, but CO_2 is only a small fraction (3–5 % by mass) of raw natural gas (COGCC, 2011), and constitutes only a negligible fraction (< 0.1 %) of total Weld/Larimer county CO_2 emissions, based on the CFRPS estimates. This suggests that while emissions of CH_4 and CO_2ff likely stem from separate processes, there is sufficient co-location of sources such that air mass mixing prior to sampling has led to good correlations between these two gases in the BAO record. Further evidence of this can be found in a consideration of multiple tracer/CO_2ff ratios, as discussed below.

3.2.3 Other trace gases

To further understand the differences in emission sources between the two wind sectors, we consider the tracer/CO_2ff ratios for a number of additional gases. Figure 6 shows the difference in median tracer/CO_2ff ratios for CO, C_2H_2, CH_4, C_3–C_5 alkanes, and benzene when winds are from the N/E and S sectors. Like CO, C_2H_2 is known to be emitted in industrialized and urban regions primarily from combustion sources (Whitby and Altwicker, 1978), while the

other gases are emitted either from non-combustion sources (C_3H_8, $n-C_4H_{10}$, and $n-C_5H_{12}$) or from a combination of sources (C_6H_6 and i-C_5H_{12}). Both CO and C_2H_2 (relative to CO_2ff) show no appreciable dependence on wind direction in our data, suggesting that both gases are emitted primarily from combustion processes that are common to Weld/Larimer counties and the Denver metro counties. The median ratio of C_2H_2 enhancement to CO_2ff observed at BAO (N/E and S combined) is 44.5 (40.7–51.8) ppt ppm^{-1} (16th–84th percentile range) ($r^2 = 0.79$, $n = 85$), which is consistent with observations from two previous studies in different US locations: 52 (45–59) ppt ppm^{-1} downwind of Sacramento, CA (Turnbull et al., 2011) and 45.9 (28.6–102.9) ppt ppm^{-1} off the east coast of the United States during winter (Miller et al., 2012). This consistency suggests a relative insensitivity of this ratio to a particular mix of emission type across the United States, an important criterion if one were to consider using C_2H_2 as a proxy for CO_2ff in the absence of $\Delta^{14}CO_2$ observations. However, the large spread observed in the enhancement ratio off the eastern US coast by Miller et al. (2012) (as reflected by the 16th and 84th percentiles of the distribution of observed ratios) suggests that there can be more variability in this ratio than indicated by the range of median values alone. Further, biomass burning can be a significant source of C_2H_2, likely impacting the C_2H_2/CO_2ff ratio in different regions at different times of year and from one year to the next. Additional research is required to better evaluate the potential for using C_2H_2 as a secondary CO_2ff tracer and whether it would prove advantageous over the use of CO (Turnbull et al., 2006; Levin and Karstens, 2007), which may be problematic in locations where significant in situ CO production results from VOC oxidation.

As with CH_4, there are significant differences in the tracer/CO_2ff enhancement ratios for the C_3–C_5 alkanes and benzene with wind direction, which suggests that enhanced emissions of these chemicals in the N/E are associated with gas and oil operations (Bar-Ilan et al., 2008a, b; Pétron et al., 2012). In general, ratios of C_3–C_5 alkanes are enhanced relative to CO_2ff by about a factor of 4–5 in the N/E wind sector compared to the S wind sector. Benzene is enhanced in the N/E wind sector compared to the S wind sector by a factor of 1.5. Despite the significant non-combustion sources of the VOCs related to gas and oil production, we see very good correlations of these species with CO_2ff in air arriving from the N/E ($r^2 > 0.71$, except for C_3H_8 for which $r^2 = 0.51$ and 0.61 for N/E and S, respectively) – an indication of integration of emissions by air mass mixing or substantial co-location of combustion sources with oil and gas operations. The enhancement of the alkane/CO_2ff ratios suggests, at least qualitatively, that a significant portion of the CH_4 detected at BAO stems from activities related to the oil and gas industry (Pétron et al., 2012), since agricultural emissions of CH_4 are not expected to be associated with emissions of C_3–C_5 alkanes.

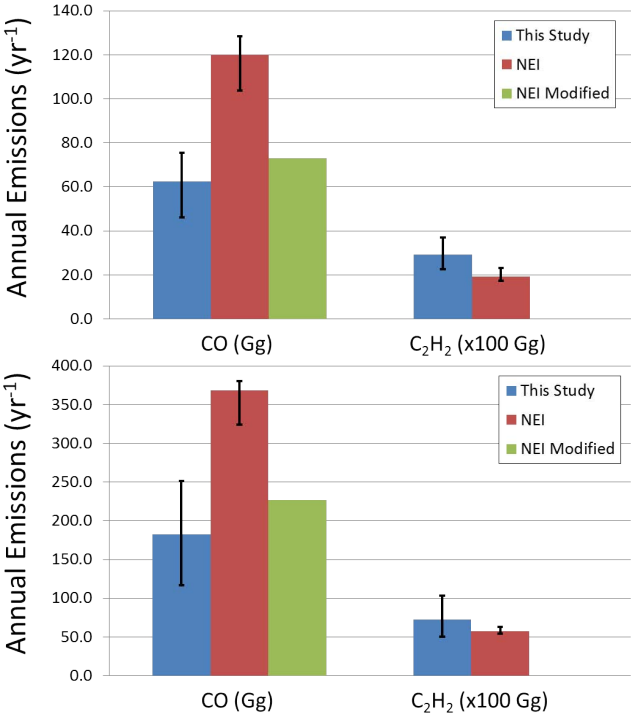

Fig. 7. Emissions estimates of CO and C_2H_2 from Weld/Larimer counties (top) and the Denver metro counties (bottom). Top-down emissions, calculated using Eq. (4), are shown as blue bars, with uncertainties given as described in Sect. 3.3. Bottom-up emissions estimates from the NEI (2005 for C_2H_2 and 2008 for CO) inventory (red) are included for comparison for each species, as well as a modified bottom-up CO inventory as described in the text. Note the differences in units for the two trace gases.

3.3 Estimating emission magnitudes

From the observations described above as well as those reported in the CFRPS, it is clear that air sampled at the BAO tall tower is strongly influenced by emissions on local-to-regional scales ($\sim 10^3$ - $\sim 10^5$ km^2). Changes in wind direction at the site result in these local emissions coming from one of two primary source regions: (1) gas and oil operations to the north and east and (2) the Denver metro region to the south. Given the distinct geographical separation of sources, we use the wind sector specific observations, in conjunction with county-level CO_2 emissions from the Vulcan data product (Gurney et al., 2009) as a means of estimating emissions for these trace gases using a tracer ratio approach.

$$E_x = E_{CO_2ff}\,(1 + \alpha\,/\,100)\,R \qquad (4)$$

Equation (4) describes the annual average top-down emissions for a series of trace gases (E_x). For reasons described below in Sect. 3.3.1, in this study we apply Eq. (4) to estimate emission magnitudes for CO and C_2H_2 only. In Eq. (4), R is the median observed tracer/CO_2ff ratio, E_{CO_2ff} is the annual average Vulcan CO_2ff emission rate for the region of

interest, and α is a scaling factor that is designed to account for changes in emissions from the emission base year to the observation period. For CO_2ff emissions, this factor is equal to the change in emissions (expressed as a %) for the EIA inventory for Colorado between 2002 (the Vulcan base year) and the most current EIA inventory year, 2009. Equation (4) is applied independently to the N/E and S wind sectors for each tracer, with R calculated for the N/E and S wind sectors paired with E_{CO_2ff} estimates for Weld/Larimer counties and the metro Denver counties, respectively. Since α is based on state wide changes in E_{CO_2ff}, this scaling factor is equivalent for both wind sectors. Tracer/CO_2ff ratios (R) are calculated as discussed in Sect. 3.2. Tables 1 and 3 summarize the parameters used to calculate E_x for Weld/Larimer counties and the Denver metro counties. Note that after applying the wind direction, wind speed, and low CO_2ff cut-off filters to the dataset there are more accepted measurements in the dataset during winter than summer, and thus any seasonal bias in the observed value R would lead to winter emissions being over-represented in the estimates of E_x. From the available data, however, we can detect no significant differences (with respect to the 2σ confidence intervals) in R with season for the two gases considered. Additionally, we do not consider potential diurnal or day-of-week variability in emissions in this analysis. Since all the samples were collected at the same time of day – within 30 min of 12:30 local time, the derived emissions and emission ratios will be biased towards daytime (vs. nighttime) emissions. Weekends are slightly over sampled in this dataset (2.5 weekend samples for every 7 total samples) which could lead to a slight bias towards weekends in the annual emissions estimates; however, we do not find any statistically significant weekday-to-weekend differences in the tracer/CO_2ff ratios.

Uncertainties in R (as described in Sect. 3.2), E_{CO_2ff}, and α are considered in the estimation of top-down emissions. The scaling term, α, is 2.8 % for the state of Colorado according to the EIA inventory. While this scaling term indicates almost no change between 2002 and 2009 emissions, in actuality, EIA emissions increased by 9 % by 2007 and then decreased over the next 2 yr (presumably related to the economic downturn in the United States during this period). Similar trends are observed in the county level Vulcan emissions over this time period, though the peak year in both Denver Metro and Weld/Larimer counties occurs earlier than 2007. Using changes in the annual EIA-based Colorado emissions to scale the Denver Metro and Weld/Larimer Vulcan02 estimates, gives, in general, very good agreement with the Vulcan estimates for these counties from 2003–2008 (to within 10 % for any given year and about 5 % on average). The Vulcan02 uncertainties (1σ) for the annual emission estimates from individual counties considered here are of similar order, ranging from 4.6 % to 10.6 %, (K. Gurney, unpublished results) with less uncertainty associated with the combined larger county "sectors" that we use in our wind sector analysis. Doubling these uncertainties (to be consistent with our 2σ analysis) for the two wind sectors results in differences from the central estimate of 7 % (upper estimate) and 11 % (lower estimate) for Weld/Larimer counties and 7 % (upper) and 10 % (lower) for the Denver metro counties. We therefore assign a conservative uncertainty of $\pm$ 20 % to the scaled bottom-up CO_2ff emissions estimates in this analysis, in which includes both uncertainty in both E_{CO_2ff} and α.

It should be noted that the Vulcan estimates may include emissions of modern (non-fossil) CO_2 from the on-road sector in locations where biofuels (ethanol) are used, including Colorado, which would lead to a positive bias in E_{CO_2ff}, and therefore, E_x. This bias would scale directly with the fraction of total CO_2ff (all sectors) in the Vulcan estimate that is from biofuels. For some perspective, a fleet-wide 15 % biofuel blend in the on-road sector (33 % of the total CO_2ff emissions in the region; see Table 2) would result in a +5 % bias in our estimates of E_x, which we consider small compared to other uncertainties. This would be roughly equivalent to assigning a value of −950‰ (rather than -1000‰) for Δ^{14}_{ff} in our derived CO_2ff estimate.

The calculated top-down emission magnitude estimates (E_x) are given as a central estimate or 'best guess' for the annual emissions plus 95 % confidence intervals calculated by propagation of the uncertainties described above. The bootstrap determination of uncertainties for the enhancement ratio provides a reasonable approximation of the impact of the variability of the tracer/CO_2ff ratios. Figure 7 summarizes the top-down estimates and confidence intervals (whiskers), along with the available bottom-up estimates, for CO and C_2H_2 for each wind sector.

3.3.1 Spatial considerations

Additional uncertainty in E_{CO_2ff} arises as a result of our assumptions regarding the geographic footprint (area of emissions) influencing the observations. Obviously, the emissions influencing the observations are not strictly confined to the county boundaries that we have selected, based on the simple wind sector analysis. This matters only to the extent that the spatial distribution of tracer/CO_2ff emission ratios varies between the presumed footprint and the actual footprint. This may be an issue especially for emissions estimates in the N/E wind sector where we expect VOC and CH_4 emissions from the DJB to be primarily confined to within Weld County while CO_2 emissions are likely significant over a larger spatial scale. For example, there are significant CO_2 emissions along the I-25 corridor (in Larimer County) to the north of BAO, where there are relatively few active gas wells (see Fig. 1). Further, whereas CO_2ff emissions are significant in both Weld (55 %) and Larimer (45 %) counties (according to Vulcan08), the vast majority (∼99.8 %) of natural gas and oil production (and, presumably, associated emissions) in the two counties is confined to Weld County (COGCC, 2011). Thus, the top-down emissions estimates of the trace gases from oil and gas production will be sensitive to our

assumptions regarding the location and scale of areas influencing the observations: specifically, whether the observations are influenced by emission fluxes from southwest Weld County only or from a larger area that extends into the eastern part of Larimer County or other locations where CO_2ff emissions are significant. Conversely, for CO and C_2H_2, the consistency in the enhancement ratio across all wind sectors supports the contention that the emissions estimates of these tracers are insensitive to presumptions about the precise area of emissions influencing the observations. Thus, we contend that the approach outlined above provides robust emission estimates for these two gases.

Because our analysis of trace gas emissions related to the oil and gas industry in the N/E wind sector is expected to be sensitive to the uncertainty in the spatial footprint of observations, we refrain from estimating absolute emission rates for the trace gases related specifically to the oil and gas industry in Weld County (CH_4, benzene, and the C_3–C_5 alkanes). Reliable estimation of emissions from this critically important sector is a matter of ongoing research, using a variety of observational platforms. Improved transport models that can accurately represent and account for the unique topography and meteorology of the Colorado Front Range will also be required, whether using a tracer/tracer approach or inverse techniques. A more in depth study of the relationship between observed CO_2ff at BAO and trace gases linked to the oil and gas sector is planned for a future publication.

3.3.2 Carbon monoxide emission estimate

We estimate annual CO emissions (shown in Fig. 7) to be 62.4 (46.0–75.5) Gg yr^{-1} CO for Weld/Larimer counties and 182.5 (116.8–251.2) Gg yr^{-1} CO for the metro Denver counties. The NEI08 estimates for these regions are 120.1 Gg CO and 368.2 Gg yr^{-1} CO, corresponding to overestimates by a factor of 1.9 and 2.0 for Weld/Larimer and metro Denver counties, respectively (Fig. 7). Our analysis indicates that total emissions for the two regions are overestimated by a factor of 2.2 (1.8–2.9) in the NEI08 bottom-up inventory. These values are consistent with prior studies evaluating the accuracy of the NEI08 (and prior versions) CO emissions (Parrish, 2006; Hudman et al., 2008; Miller et al., 2008; Turnbull et al., 2011; Miller et al., 2012).

Comparing the results of different studies where radiocarbon observations were used to derive CO/CO_2ff ratios provides some insight into the ubiquity of the overestimate of CO emissions in the NEI inventory. A survey of observed CO/CO_2ff ratios from different locations, including Sacramento, CA (Turnbull et al., 2011), Denver (Turnbull et al., 2006; Graven et al., 2009), Irvine, CA (Djuricin et al., 2010), and off the eastern coast of the United States (Miller et al., 2012), reveals regional differences in the comparison between observations and bottom-up estimates (Fig. 5). The observations from the eastern seaboard of the United States point to an overestimate of NEI08 CO emissions (Miller et al., 2012), while both California-based studies find that the observed CO/CO_2ff ratio closely matches the estimates from California bottom-up inventories (Fig. 5). The Sacramento results were found to be in agreement with the California Air Resources Board (CARB) 2008 inventory, but the NEI05 inventory was high by about a factor of two (Turnbull et al., 2011). From our analysis, it appears as though this overestimate in the NEI inventory for California has been corrected in the 2008 release, perhaps a result of adopting the CARB estimates, as previously suggested by Turnbull et al. (2011). Similarly, the observations in Irvine (Djuricin et al., 2010) are in good agreement with the NEI08 inventory for the LA Basin (Los Angeles, Orange County, San Bernardino, and Riverside counties). From the BAO observations and those off the east coast of the US, it appears as though corrections were not made for the rest of the country.

As with the previous Denver observations, the Sacramento and Irvine observations are representative of shorter time periods: the Sacramento observations were compiled from linear correlations of 10 samples collected during 2 aircraft flights, while the Irvine observations were from 3 discrete samples collected over a few different months at a surface site on the campus of UC Irvine. The Miller et al. study provides a longer term average, similar to the BAO observations, but is more representative of northeast US regional-scale ($\sim 10^5$–$\sim 10^6$ km^2) sources rather than the local-to-regional ($\sim 10^3$–$\sim 10^5$ km^2) influence at BAO. Given the large differences in time and space scales relevant to each of these studies, the comparisons of CO/CO_2ff ratios in the various locations are not necessarily conclusive. However, as we will discuss in Sect. 4, we find that a closer inspection of the NEI08 inventory reveals a significant difference in the CO inventory in California vs. Colorado that is not supported by observations.

In situ production or loss of CO could also potentially bias these results. The most likely scenario would be the production of CO from the oxidation of VOCs by OH (Griffin et al., 2007) which can be significant in some locations, especially during summer when oxidation rates are intensified and biogenic VOC emissions are high (Turnbull et al., 2006). At BAO, we do not see an appreciable difference in the CO/CO_2ff ratio from winter to summer, which suggests little photochemical influence on CO abundance at BAO. The atmospheric lifetime of CO is sufficiently long ($\sim$50 days) that consumption of CO by OH is also likely to be negligible in this analysis.

3.3.3 Acetylene emission estimate

Acetylene emissions are estimated to be 0.29 (0.23–0.37) Gg yr^{-1} in Weld/Larimer counties and 0.73 (0.51–1.0) Gg yr^{-1} in the Denver Metro counties. These values are higher than the bottom-up estimates by factors of 1.5 (1.2–1.9) and 1.3 (0.9–1.8) for Weld/Larimer and Denver metro, respectively (Fig. 7). Nonlinearity issues with the

C_2H_2 measurements may result in a positive bias for our emission estimates by as much as 12 % (see Sect. 2.3), but this is not enough to bring the top-down and bottom-up estimates into agreement. In contrast to carbon monoxide, there has been very little evaluation of C_2H_2 emissions inventories in the United States. Warneke et al. (2007) compared the C_2H_2 : CO ratio from observations in Boston, New York, and Los Angeles to that in the NEI99 emissions database, and found the ratio to be underestimated in each location, suggesting a systematic underestimation of acetylene emissions by the NEI database. However, it is unclear whether this underestimation of the C_2H_2 : CO ratio is a result of an underestimate of C_2H_2 or an overestimate of CO (as detailed above). Using observations of $^{14}CO_2$, the C_2H_2 inventory can be evaluated independently of any biases in the CO emissions inventory. There have been two recent examples comparing top-down estimates of C_2H_2 emissions in the United States to bottom-up inventories using $^{14}CO_2$ observations: Miller et al. (2012) estimated C_2H_2 emissions for the entire United States (assuming northeast ratios were nationally representative) and found relatively good agreement (within 6 %) with the NEI05 C_2H_2 emissions inventory (the same gridded inventory used for comparison in this study and described above); Turnbull et al. (2011) published a comparison of C_2H_2:CO_2ff ratios from observations of the Sacramento urban plume with that calculated from bottom-up inventories and found a ∼30 % underestimate of C_2H_2 in the NEI05 inventory for Sacramento, CA. Both of these estimates, it should be noted, were made relative to the same C_2H_2 standard scale as in our estimates. Additional $^{14}CO_2$ observations co-measured with C_2H_2 in more locations and comparison with contemporaneous NEI05 values are required to come to any definitive conclusions regarding the accuracy of C_2H_2 emissions in the NEI05 database. The use of C_2H_2 as a secondary fossil fuel tracer or a proxy for CO_2ff seems promising, however, given the limited evaluation of C_2H_2 emission sources in the literature as of today, further studies are recommended.

4 Implications for Carbon Monoxide Inventory

As discussed in Sect. 3.3.2, our observations and evaluation of the NEI08 inventory are consistent with prior findings that CO emissions are overestimated at the national level in previous versions of the NEI inventory (Parrish, 2006; Hudman et al., 2008; Miller et al., 2008). There is evidence, albeit from a limited number of samples, that the California county-level bottom-up emissions of CO more accurately reflect the emissions estimated from atmospheric observations (Fig. 4). This provides the motivation to investigate whether there are fundamental differences in the methods for compiling the bottom-up CO inventory in California vs. Colorado, as well as in other states.

An analysis of the on-road sector CO (NEI08) and CO_2ff (Vulcan08) emissions in comparison with the on-road observations of tail-pipe emissions of CO by Bishop and Stedman (2008) in Denver and Los Angeles (Fig. 8) suggests that NEI08 CO emissions in the on-road sector, specifically, are biased high in Colorado. These on-road observations show only very small differences between the CO:fuel-burnt ratio (and therefore the CO/CO_2 ratio) emitted from vehicles in Denver (in 2006) and Los Angeles (in 2008). The CO:fuel-burnt ratios observed in the two cities correspond to CO/CO_2 emission ratios of 16 ppb ppm^{-1} (Denver in 2006) and 18 ppb ppm^{-1} (Los Angeles in 2006). In Los Angeles, the observed ratio (Bishop and Stedman, 2008) closely resembles the bottom-up ratio of 17 ppb ppm^{-1} calculated from the NEI08 and Vulcan08 inventories for the on-road sector only; however, the on-road sector bottom-up ratio (NEI08:Vulcan08) for Denver is 40 ppb ppm^{-1}, which is 2.5 times the observed ratio (Bishop and Stedman, 2008). Similarly, in Weld/Larimer counties the bottom-up ratio is 43 ppb ppm^{-1} and US-wide it is 38 ppb ppm^{-1}. It should be noted that the on-road CO emissions in California are estimated using a different mobile source model, EMFAC2007 (EMFAC, hereafter) (CARB, 2007) than that used for the rest of the United States, MOBILE6.2 (MOBILE, hereafter) (EPA, 2012b). In light of our comparison of CO/CO_2ff observations between California and other regions, and given the Bishop and Stedman (2008) observations in comparison with the on-road sector bottom up inventories, it appears likely that the MOBILE CO emission factor outputs are biased high relative to the EMFAC model.

This is also consistent with a recent comparison (Fujita et al., 2012) of these two mobile source models, along with the MOVES2010a (MOVES, hereafter) model, which was recently adopted by the EPA (EPA, 2010). This study showed that MOBILE emission factor outputs are biased high relative to the EMFAC and MOVES outputs, both of which showed close agreement with observations in a Los Angeles tunnel study. This analysis showed that CO was overestimated by the MOBILE model by a factor of 1.6–2.0 across a range of temperatures and traffic conditions and was found to be relatively insensitive to whether emission control programs were included in the model inputs. Both EMFAC and MOBILE use a region-wide average driving schedule and speed to compile emission factors for different vehicle types and model years, while MOVES uses a more specific approach, where emission factors are calculated for different speed and power bins. The consistency between MOVES, EMFAC, and the observations detailed in Fujita et al. (2012), suggests that the general framework of the MOBILE model for scaling up emission factors from individual vehicles for an average driving schedule, which is essentially the same as that used by the EMFAC model, is not the issue. Rather, the emission ratios associated with individual vehicle types and model years need to be adjusted. A separate study by the Federal Highway Administration Resource Center (Claggett

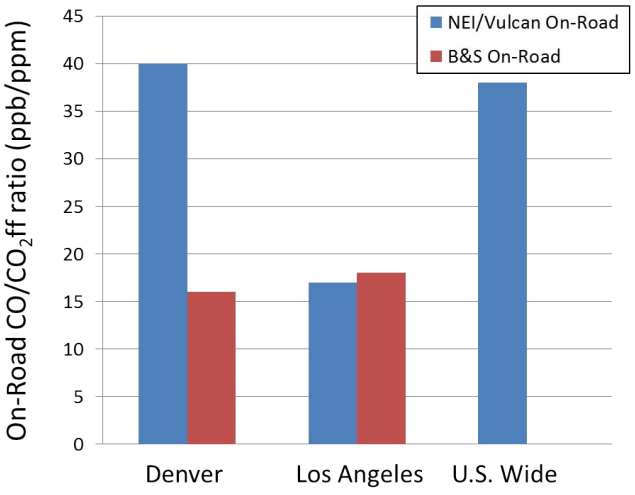

Fig. 8. On-road sector CO/CO_2ff emission ratios derived from the tailpipe observations of Bishop and Stedman (2008) (B&S, red) and from the sector-specific NEI08 CO and Vulcan 2.2 CO_2 emissions estimates (blue) for Denver, Los Angeles, and the US.

and Houk, 2008) also analyzed differences in emission factor outputs by the EMFAC and MOBILE models and found that across a spectrum of average vehicle speeds for identical vehicle fleets in 2010 (a future scenario in the 2008 study), the MOBILE model CO emission factors were higher than the EMFAC output by 50–300 %, depending on the average vehicle speed.

With the EPA soon to adopt MOVES2010a for the NEI, and given the analysis of Fujita et al. (2012), future releases of the NEI inventory can be expected to produce more accurate estimates of CO emissions for Colorado and the rest of the US. However, continued evaluations of these mobile source models should be performed alongside observations such as those presented here, as well as those from Bishop and Stedman (2008) and Fujita et al. (2012).

We derive a modified bottom-up CO estimate for the Denver metro counties and Weld/Larimer counties in which the NEI08 on-road sector CO emission rate is replaced with a new estimate calculated from the Vulcan08 on-road sector CO_2 emission rate and the observed on-road sector CO/CO_2 ratio of 16 ppb ppm^{-1} from Bishop and Stedman (2008). This new estimate, shown in Fig. 7 and labeled as "Modified NEI", brings the top-down and bottom-up values to within 24 % for the Denver metro counties and to within 18 % for Weld/Larimer counties. The remaining discrepancy between these modified estimates and the observations could be a result of some combination of: (1) diesel vehicles that contribute significantly to the on-road sector CO_2 emissions but are not a significant source of CO; and (2) a reduction in the CO-to-fuel-burnt emission ratio between 2008 and 2009–2010. Additionally, this crude scaling exercise does not take into account changes in the CO/CO_2 emission ratio during "cold starts", which likely introduces significant variability at smaller spatial scales and shorter temporal scales. With these caveats acknowledged, scaling-up of this modified CO inventory reduces the total anthropogenic source of CO in the United States from 60 Tg yr^{-1} to 39 Tg yr^{-1}, close to the 60 % reduction suggested by Hudman et al. (2008) for anthropogenic CO emissions in the United States and close to the national $^{14}CO_2$ based estimate of 41 (33–53) Tg yr^{-1} (Miller et al., 2012).

5 Summary and conclusions

We have analyzed 145 whole air samples for $\Delta^{14}CO_2$ collected across 15 months at the NOAA BAO tall tower in Erie, Colorado. Air sampled at this site is heavily impacted by emissions from a variety of local sources including urban, rural, and industrial activities. The oil and gas industry, in particular, was found to contribute to enhancements in a number of industry-related trace gases relative to fossil fuel CO_2 when the tower is downwind of oil and gas activities, which are concentrated in Weld County to the north and east of the sampling tower, although the relative contribution of other sources of CH_4 in this sector were not determined. The observed enhancements suggest that emissions of CH_4, C_3–C_5 alkanes, and benzene (relative to CO_2ff emissions) are a factor of 3, ∼4–5, and 1.5 greater, respectively, in air masses travelling from Weld and Larimer counties (north and east) over those originating from the Denver metro counties (south).

With the availability of a spatially resolved bottom-up CO_2ff emissions data product from the Vulcan Project, we are able to take a tracer/tracer approach using CO_2ff, derived from $\Delta^{14}CO_2$ observations, as a reference tracer, to critically evaluate the accuracy of the bottom-up emissions inventories for CO and C_2H_2. For these two gases, we find no significant differences in apparent emission ratio relative to CO_2ff between the metro Denver region and Weld/Larimer counties, which suggests that top-down emissions estimates are largely insensitive to the assumptions about the sample footprint. We show that for both Weld/Larimer counties and the Denver metro counties, C_2H_2 is underestimated in the NEI05 inventory by a factor of about 0.66 while CO is overestimated in the NEI08 inventory by a factor of ∼2. From the NEI08 CO and Vulcan08 CO_2ff emissions estimates, we calculate that the average emission factor from on-road gasoline vehicles is ∼40 ppb CO ppm^{-1} CO_2 for the region, while our observations suggest an emission ratio of 16 ppb ppm^{-1} for these vehicles.

For the trace gases originating from activities of the oil and gas industry to the north and east of the sampling tower, the primary barrier to estimating absolute emissions is the uncertainty in the spatial extent of the observation footprint, and therefore, the precise reference emissions value for CO_2ff. Weld and Larimer counties present an extreme case, in this regard, where emissions related to the oil and

gas industry are confined to a well-defined region within a larger region of significant CO_2ff emissions from mobile sources and where there is significant spatial heterogeneity in tracer/CO_2ff emission ratios. The incorporation of a reliable mesoscale atmospheric transport model into the analysis may allow for a more reliable estimation of absolute emissions for these gases. The increasing economic importance of the natural gas industry in the US and the uncertain climate and health ramifications provides strong motivation for a detailed study of the atmospheric transport in this region so that the $\Delta^{14}CO_2$ observations at the BAO tower may be used to derive accurate emissions estimates of CH_4.

Supplementary material related to this article is available online at http://www.atmos-chem-phys.net/13/11101/2013/acp-13-11101-2013-supplement.pdf.

Acknowledgements. The authors would like to acknowledge Paula Zermeño (CAMS), Shane Bradshaw (CAMS), and Chad Wolak (INSTAAR) for their contributions to $^{14}CO_2$ sample preparation, to C. Siso for analysis of the non-methane hydrocarbons, and to D. Kitzis for the preparation of the NWT reference cylinders. Funding was provided by DOE's Office of Biological and Environmental Research and NOAA. A portion of this work was performed under the auspices of the US Department of Energy by Lawrence Livermore National Laboratory under Contract DE-AC52-07NA27344.

Edited by: R. McLaren

References

Andres, R. J., Boden, T. A., Breon, F. M., Ciais, P., Davis, S., Erickson, D., Gregg, J. S., Jacobson, A., Marland, G., Miller, J., Oda, T., Olivier, J. G. J., Raupach, M. R., Rayner, P., and Treanton, K.: A synthesis of carbon dioxide emissions from fossil-fuel combustion, Biogeosciences, 9, 1845–1871, doi:10.5194/bg-9-1845-2012, 2012.

Andrews, A. E., Kofler, J. D., Trudeau, M. E., Williams, J. C., Neff, D. H., Masarie, K. A., Chao, D. Y., Kitzis, D. R., Novelli, P. C., Zhao, C. L., Dlugokencky, E. J., Lang, P. M., Crotwell, M. J., Fischer, M. L., Parker, M. J., Lee, J. T., Baumann, D. D., Desai, A. R., Stanier, C. O., de Wekker, S. F. J., Wolfe, D. E., Munger, J. W., and Tans, P. P.: CO_2, CO and CH_4 measurements from the NOAA Earth System Research Laboratory's Tall Tower Greenhouse Gas Observing Network: instrumentation, uncertainty analysis and recommendations for future high-accuracy greenhouse gas monitoring efforts, Atmos. Meas. Tech. Discuss., 6, 1461–1553, doi:10.5194/amtd-6-1461-2013, 2013.

Atkinson, R., Baulch, D. L., Cox, R. A., Crowley, J. N., Hampson, R. F., Hynes, R. G., Jenkin, M. E., Rossi, M. J., and Troe, J.: Evaluated kinetic and photochemical data for atmospheric chemistry: Volume II – gas phase reactions of organic species, Atmos. Chem. Phys., 6, 3625-4055, doi:10.5194/acp-6-3625-2006, 2006.

Bar-Ilan, A., Moore, T., Gribovicz, L., Sgamma, K., Pollack, A., and Henderer, D.: Development of baseline 2006 emissions from oil and gas activity in the Denver-Julesburg Basin, WRAP Phase III report http://www.wrapair.org/forums/ogwg/PhaseIII_Inventory.html, 34 pp., 2008a.

Bar-Ilan, A., Moore, T., Gribovicz, L., Sgamma, K., Pollack, A., and Henderer, D.: Development of 2010 oil and gas emissions projections for the Denver-Julesburg Basin, WRAP Phase III report http://www.wrapair.org/forums/ogwg/PhaseIII_Inventory.html, 26 pp., 2008b.

Bishop, G. A. and Stedman, D. H.: A decade of on-road emissions measurements, Environ. Sci. Technol., 42, 1651–1656, 2008.

Brennan, P. J.: Los Angeles Wildfire Sends Pollution as Far as Denver, Bloomberg, http://www.bloomberg.com/apps/news?pid=_newsarchive&sid=_aJrSkTFs1dL4, (last access: 2009), 2009.

California Air Resources Board Mobile Sources Emissions Inventory, available at: http://www.arb.ca.gov/msei/onroad/latest_version.htm (last access: 10 October 2012), 2007.

Claggett, M. and Houk, J.: Comparing MOBILE6.2 and EMFAC2007 Emission Factors, Transp. Res. Record, 51–57, doi:10.3141/2058-07, 2008.

COGCC: Colorado Oil and Gas Information System Data Base accessible at http://cogcc.state.co.us (last access: 14 June 2011), 2011.

Conway, T. J., Tans, P. P., Waterman, L. S., and Thoning, K. W.: Evidence for Interannual Variability of the Carbon-Cycle from the National-Oceanic-and-Atmospheric-Administration Climate-Monitoring-and-Diagnostics-Laboratory Global-Air-Sampling-Network, J. Geophys. Res. Atmos., 99, 22831–22855, 1994.

Currie, K. I., Brailsford, G., Nichol, S., Gomez, A., Sparks, R., Lassey, K. R., and Riedel, K.: Tropospheric (CO_2)–C_{14} at Wellington, New Zealand: the world's longest record, Biogeochem., 104, 5–22, 2011.

Djuricin, S., Pataki, D. E., and Xu, X. M.: A comparison of tracer methods for quantifying CO_2 sources in an urban region, J. Geophys. Res.-Atmos., 115, D11303, doi:10.1029/2009JD012236, 2010.

Dlugokencky, E. J., Steele, L. P., Lang, P. M., and Masarie, K. A.: The Growth-Rate and Distribution of Atmospheric Methane, J. Geophys. Res. Atmos., 99, 17021–17043, 1994.

EPA: Official release of the MOVES2010 motor vehicle emissions model for emission inventories in SIPs and tranportation conformity, Fed. Regist., 75, 9411–9414, 2010.

EPA: Speciate Software Download Site: http://www.epa.gov/ttnchie1/software/speciate/ (last access: 19 June 2012), 2011.

EPA: MOBILE6 Vehicle Emission Modeling Software: http://www.epa.gov/oms/m6.htm (last access: 10 October 2012), 2012.

Fujita, E. M., Campbell, D. E., Zielinska, B., Chow, J. C., Lindhjem, C. E., DenBleyker, G. A., Bishop, G. A., Schuchmann, B. G., Stedman, D. H., and Lawson, D. R.: Comparison of the MOVES2010a, MOBILE6.2, and EMFAC2007 mobile source emission models with on-road traffic tunnel and remote sensing measurements, J. Air Waste Manage. Assoc., 62, 1134–1149, doi:10.1080/10962247.2012.699016, 2012.

Godwin, H.: Half-Life of Radiocarbon, Nature, 195, 984, doi:10.1038/195984a0, 1962.

Graven, H. D. and Gruber, N.: Continental-scale enrichment of atmospheric $^{14}CO_2$ from the nuclear power industry: potential impact on the estimation of fossil fuel-derived CO_2, Atmos. Chem. Phys., 11, 12339–12349, doi:10.5194/acp-11-12339-2011, 2011.

Graven, H. D., Guilderson, T. P., and Keeling, R. F.: Methods for high-precision C_{14} AMS measurement of atmospheric CO_2 at LLNL, Radiocarbon, 49, 349–356, 2007.

Graven, H. D., Stephens, B. B., Guilderson, T. P., Campos, T. L., Schimel, D. S., Campbell, J. E., and Keeling, R. F.: Vertical profiles of biospheric and fossil fuel-derived CO_2 and fossil fuel CO_2: CO ratios from airborne measurements of Delta(14)C, CO_2 and CO above Colorado, USA, Tellus B, 61, 536–546, 2009.

Graven, H. D., Guilderson, T. P., and Keeling, R. F.: Observations of radiocarbon in CO_2 at seven global sampling sites in the Scripps flask network: Analysis of spatial gradients and seasonal cycles J. Geophys. Res., 117, D02303, doi:10.1029/2011JD016535, 2012a.

Graven, H. D., Guilderson, T. P., and Keeling, R. F.: Observations of radiocarbon in CO_2 at La Jolla, California, USA 1992–2007: Analysis of the long-term trend, J. Geophys. Res., 117, D02302, doi:10.1029/2011JD016533, 2012b.

Griffin, R. J., Chen, J. J., Carmody, K., Vutukuru, S., and Dabdub, D.: Contribution of gas phase oxidation of volatile organic compounds to atmospheric carbon monoxide levels in two areas of the United States, J. Geophys. Res.-Atmos., 112, D10S17, doi:10.1029/2006jd007602, 2007.

Gurney, K. R., Mendoza, D. L., Zhou, Y. Y., Fischer, M. L., Miller, C. C., Geethakumar, S., and Du Can, S. D.: High Resolution Fossil Fuel Combustion CO_2 Emission Fluxes for the United States, Environ. Sci. Technol., 43, 5535–5541, 2009.

Gurney, K. R., Chandrasekaran, V., Mendoza, D. L., and Geethakumar, S.: Quantification of uncertainty associated with NACP high resolution fossil fuel CO_2 emissions: updates, challenges and future plans, North American Carbon Program All-Inverstigators Meeting, New Orleans, LA, available at: http://www.nacarbon.org/meeting_ab_presentations/2011/2011_Feb03_AM_Gurney_63.ppt, last access: 18 October 2013, 2011.

Hsueh, D. Y., Krakauer, N. Y., Randerson, J. T., Xu, X. M., Trumbore, S. E., and Southon, J. R.: Regional patterns of radiocarbon and fossil fuel-derived CO_2 in surface air across North America, Geophys. Res. Lett., 34, L02816, doi:10.1029/2006GL027032, 2007.

Hudman, R. C., Jacob, D. J., Cooper, O. R., Evans, M. J., Heald, C. L., Park, R. J., Fehsenfeld, F., Flocke, F., Holloway, J., Hubler, G., Kita, K., Koike, M., Kondo, Y., Neuman, A., Nowak, J., Oltmans, S., Parrish, D., Roberts, J. M., and Ryerson, T.: Ozone production in transpacific Asian pollution plumes and implications for ozone air quality in California, J. Geophys. Res., 109, D23S10, doi:10.1029/2004JD004974, 2004.

Hudman, R. C., Murray, L. T., Jacob, D. J., Millet, D. B., Turquety, S., Wu, S., Blake, D. R., Goldstein, A. H., Holloway, J., and Sachse, G. W.: Biogenic versus anthropogenic sources of CO in the United States, Geophys. Res. Lett., 35, L04801, doi:10.1029/2007GL032393, 2008.

Lee, B. H., Munger, J. W., Wofsy, S. C., and Goldstein, A. H.: Anthropogenic emissions of nonmethane hydrocarbons in the northeastern United States: Measured seasonal variations from 1992–1996 and 1999–2001, J. Geophys. Res.-Atmos., 111, D20307, doi:10.1029/2005JD006172, 2006.

Lehman, S. J., Miller, J. B., Wolak, C., Southon, J., Tans, P. P., Montzka, S. A., Sweeney, C., Andrews, A., LaFranchi, B. W., Guilderson, T. P., Fischer, M. L., and Turnbull, J. C.: Allocation of terrestrial carbon sources using $^{14}CO_2$: measurement and modeling, Radiocarbon, 55, 1484–1495, 2013.

Levin, I. and Karstens, U. T. E.: Inferring high-resolution fossil fuel CO_2 records at continental sites from combined $^{14}CO_2$ and CO observations, Tellus B, 59, 245–250, doi:10.1111/j.1600-0889.2006.00244.x, 2007.

Levin, I. and Kromer, B.: The tropospheric (CO_2)-C_{14} level in midlatitudes of the Northern Hemisphere (1959–2003), Radiocarbon, 46, 1261–1272, 2004.

Levin, I., Kromer, B., Schmidt, M., and Sartorius, H.: A novel approach for independent budgeting of fossil fuel CO_2 over Europe by (CO_2)-C_{14} observations, Geophys. Res. Lett., 30, 2194, doi:10.1029/2003GL018477, 2003.

Levin, I., Naegler, T., Kromer, B., Diehl, M., Francey, R. J., Gomez-Pelaez, A. J., Steele, L. P., Wagenbach, D., Weller, R., and Worthy, D. E.: Observations and modelling of the global distribution and long-term trend of atmospheric $^{14}CO_2$, Tellus B, 62, 26–46, 2010.

Miller, J. B., Lehman, S. J., Montzka, S. A., Sweeney, C., Miller, B. R., Wolak, C., Dlugokencky, E. J., Southon, J., Turnbull, J. C., and Tans, P. P.: Linking emissions of fossil fuel CO_2 and other anthropogenic trace gases using atmospheric $^{14}CO_2$, J. Geophys. Res. Atmos., D08302, doi:10.1029/2011JD017048, 2012.

Miller, S. M., Matross, D. M., Andrews, A. E., Millet, D. B., Longo, M., Gottlieb, E. W., Hirsch, A. I., Gerbig, C., Lin, J. C., Daube, B. C., Hudman, R. C., Dias, P. L. S., Chow, V. Y., and Wofsy, S. C.: Sources of carbon monoxide and formaldehyde in North America determined from high-resolution atmospheric data, Atmos. Chem. Phys., 8, 7673–7696, doi:10.5194/acp-8-7673-2008, 2008.

Montzka, S. A., Myers, R. C., Butler, J. H., Elkins, J. W., and Cummings, S. O.: Global Tropospheric Distribution and Calibration Scale of Hcfc-22, Geophys. Res. Lett., 20, 703–706, 1993.

Muller, S. A., Joos, F., Plattner, G. K., Edwards, N. R., and Stocker, T. F.: Modeled natural and excess radiocarbon: Sensitivities to the gas exchange formulation and ocean transport strength, Global Biogeochem. Cy., 22, GB3011, doi:10.1029/2007GB003065, 2008.

NASA: Chemical Kinetics and Photochemical Data for Use in Atmospheric Studies Evaluation Number 15: http://jpldataeval.jpl.nasa.gov/ (last access: 28 June 2010), 2006.

Nassar, R., Napier-Linton, L., Gurney, K. R., Andres, R. J., Oda, T., Vogel, F. R., and Deng, F.: Improving the temporal and spatial distribution of CO_2 emissions from global fossil fuel emission datasets, J. Geophys. Res. Atmos., 118, 917-933, doi:10.1029/2012jd018196, 2013.

National Emissions Inventory: http://www.epa.gov/ttn/chief/eiinformation.html (last access: 26 January 2011), 2008.

Novelli, P. C., Connors, V. S., Reichle, H. G., Anderson, B. E., Brenninkmeijer, C. A. M., Brunke, E. G., Doddridge, B. G., Kirchhoff, V. W. J. H., Lam, K. S., Masarie, K. A., Matsuo, T., Parrish, D. D., Scheel, H. E., and Steele, L. P.: An internally consistent set of globally distributed atmospheric carbon monoxide mixing ratios developed using results from an intercomparison of measurements, J. Geophys. Res. Atmos., 103, 19285–19293, 1998.

Parrish, D. D.: Critical evaluation of US on-road vehicle emission inventories, Atmos. Environ., 40, 2288–2300, 2006.

Pétron, G., Frost, G., Hirsch, A. I., Montzka, S. A., Karion, A., Miller, B. R., Trainer, M., Sweeney, C., Andrews, A. E., Miller, L., Kofler, J., Ryerson, T., Patrick, L., Siso, C., Kolodzey, W., Lang, P., Dlugokencky, E., Conway, T., Novelli, P., Masarie, K., Hall, B., Guenther, D., Kitzis, D., Miller, J. B., Neff, W., Wolfe, D., and Tans, P. P.: Hydrocarbon emissions characterization in the Colorado front range – A pilot study, J. Geophys. Res. Atmos., 117, D04304, doi:10.1029/2011JD016360, 2012.

Schuur, E. A. G., Trumbore, S. E., Mack, M. C., and Harden, J. W.: Isotopic composition of carbon dioxide from a boreal forest fire: Inferring carbon loss from measurements and modeling, Global Biogeochem. Cy., 17, 1001, doi:10.1029/2001GB001840, 2003.

Stuiver, M. and Polach, H. A.: Reporting of C_{14} Data – Discussion, Radiocarbon, 19, 355–363, 1977.

Suess, H. E.: Radiocarbon Concentration in Modern Wood, Science, 122, 415–417, 1955.

Sweeney, C., Gloor, E., Jacobson, A. R., Key, R. M., McKinley, G., Sarmiento, J. L., and Wanninkhof, R.: Constraining global air-sea gas exchange for CO_2 with recent bomb (14)C measurements, Global Biogeochem. Cy., 21, GB2015, doi:10.1029/2006GB002784, 2007.

Thompson, M. V. and Randerson, J. T.: Impulse response functions of terrestrial carbon cycle models: method and application, Glob. Change Biol., 5, 371–394, 1999.

Thoning, K. W., Tans, P. P., and Komhyr, W. D.: Atmospheric Carbon-Dioxide at Mauna Loa Observatory .2. Analysis of the NOAA GMCC Data, 1974–1985, J. Geophys. Res. Atmos., 94, 8549–8565, 1989.

Turnbull, J., Rayner, P., Miller, J., Naegler, T., Ciais, P., and Cozic, A.: On the use of (14)CO_2 as a tracer for fossil fuel CO_2: Quantifying uncertainties using an atmospheric transport model, J. Geophys. Res. Atmos., 114, D22302, doi:10.1029/2009JD012308, 2009.

Turnbull, J. C., Miller, J. B., Lehman, S. J., Tans, P. P., Sparks, R. J., and Southon, J.: Comparison of (CO_2)-C_{14}, CO, and SF6 as tracers for recently added fossil fuel CO_2 in the atmosphere and implications for biological CO_2 exchange, Geophys. Res. Lett., 33, L01817, doi:10.1029/2005GL024213, 2006.

Turnbull, J. C., Lehman, S. J., Miller, J. B., Sparks, R. J., Southon, J. R., and Tans, P. P.: A new high precision $^{14}CO_2$ time series for North American continental air, J. Geophys. Res. Atmos., 112, D11310, doi:10.1029/2006JD008184, 2007.

Turnbull, J. C., Lehman, S. J., Morgan, S., and Wolak, C.: A New Automated Extraction System for (14)C Measurement for Atmospheric CO_2, Radiocarbon, 52, 1261–1269, 2010.

Turnbull, J. C., Karion, A., Fischer, M. L., Faloona, I., Guilderson, T., Lehman, S. J., Miller, B. R., Miller, J. B., Montzka, S., Sherwood, T., Saripalli, S., Sweeney, C., and Tans, P. P.: Assessment of fossil fuel carbon dioxide and other anthropogenic trace gas emissions from airborne measurements over Sacramento, California in spring 2009, Atmos. Chem. Phys., 11, 705–721, doi:10.5194/acp-11-705-2011, 2011.

US Energy Information Administration CO_2 Emissions Data: http://www.eia.gov/environment/data.cfm#summary (last access: 18 June 2012), 2012.

Van der Laan, S., Karstens, U., Neubert, R. E. M., Van der Laan-Luijkx, I. T., and Meijer, H. A. J.: Observation-based estimates of fossil fuel-derived CO_2 emissions in the Netherlands using Delta 14C, CO and 222Radon, Tellus B, 62, 389–402, 2010.

Vaughn, B. H., Miller, J. B., Ferretti, D. F., and White, J. C.: Stable isotope measurements of atmospheric CO_2 and CH4, in: Handbook of Stable Isotope Analytical Techniques, edited by: de Groot, P., Elsevier Inc., San Diego, CA, USA, 272–304, 2004.

Vay, S. A., Choi, Y., Vadrevu, K. P., Blake, D. R., Tyler, S. C., Wisthaler, A., Hecobian, A., Kondo, Y., Diskin, G. S., Sachse, G. W., Woo, J. H., Weinheimer, A. J., Burkhart, J. F., Stohl, A., and Wennberg, P. O.: Patterns of CO_2 and radiocarbon across high northern latitudes during International Polar Year 2008, J. Geophys. Res. Atmos., 116, D14301, doi:10.1029/2011JD015643, 2011.

Wallace, H. W., Jobson, B. T., Erickson, M. H., McCoskey, J. K., VanReken, T. M., Lamb, B. K., Vaughan, J. K., Hardy, R. J., Cole, J. L., Strachan, S. M., and Zhang, W.: Comparison of wintertime CO to NO_x ratios to MOVES and MOBILE6.2 on-road emissions inventories, Atmos. Environ., 63, 289–297, doi:10.1016/j.atmosenv.2012.08.062, 2012.

Warneke, C., McKeen, S. A., de Gouw, J. A., Goldan, P. D., Kuster, W. C., Holloway, J. S., Williams, E. J., Lerner, B. M., Parrish, D. D., Trainer, M., Fehsenfeld, F. C., Kato, S., Atlas, E. L., Baker, A., and Blake, D. R.: Determination of urban volatile organic compound emission ratios and comparison with an emissions database, J. Geophys. Res. Atmos., 112, D10S47, doi:10.1029/2006JD007930, 2007.

Watson, J. G., Chow, J. C., and Fujita, E. M.: Review of volatile organic compound source apportionment by chemical mass balance, Atmos. Environ., 35, 1567-1584, 2001.

Whitby, R. A. and Altwicker, E. R.: Acetylene in Atmosphere – Sources, Representative Ambient Concentrations and Ratios to Other Hydrocarbons, Atmos. Environ., 12, 1289–1296, doi:10.1016/0004-6981(78)90067-7, 1978.

Zondervan, A. and Meijer, H. A. J.: Isotopic characterisation of CO_2 sources during regional pollution events using isotopic and radiocarbon analysis, Tellus B, 48, 601–612, 1996.